

Probing the nature of rotation in the Pleiades, Alpha Persei, and Hyades clusters

C. J. HAO,^{1,2} Y. XU,^{1,2} L. G. HOU,³ S. B. BIAN,¹ Z. H. LIN,¹ Y. J. LI,¹ Y. W. DONG,^{1,2} AND D. J. LIU^{1,2}

¹*Purple Mountain Observatory, Chinese Academy of Sciences, Nanjing 210023, PR China*

²*School of Astronomy and Space Science, University of Science and Technology of China, Hefei 230026, PR China*

³*National Astronomical Observatories, Chinese Academy of Sciences, 20A Datun Road, Chaoyang District, Beijing 100101, PR China*

ABSTRACT

Unraveling the internal kinematics of open clusters is crucial for understanding their formation and evolution. However, there is a dearth of research on this topic, primarily due to the lack of high-quality kinematic data. Using the exquisite-precision astrometric parameters and radial velocities provided by *Gaia* data release 3, we investigate the internal rotation in three of the most nearby and best-studied open clusters, namely the Pleiades, Alpha Persei, and Hyades clusters. Statistical analyses of the residual motions of the member stars clearly indicate the presence of three-dimensional rotation in the three clusters. The mean rotation velocities of the Pleiades, Alpha Persei, and Hyades clusters within their tidal radii are estimated to be 0.24 ± 0.04 , 0.43 ± 0.08 , and 0.09 ± 0.03 km s⁻¹, respectively. Similar to the Praesepe cluster that we have studied before, the rotation of the member stars within the tidal radii of these three open clusters can be well interpreted by Newton's theorem. No expansion or contraction is detected in the three clusters either. Furthermore, we find that the mean rotation velocity of open clusters may be positively correlated with the cluster mass, and the rotation is likely to diminish as open clusters age.

Keywords: open clusters and associations: individual (Pleiades) – open clusters and associations: individual (Alpha Persei) – open clusters and associations: individual (Hyades) – stars: kinematics and dynamics – methods: statistical

1. INTRODUCTION

Most stars in the Milky Way are thought to form in star clusters (Lada & Lada 2003; Bressert et al. 2010; Megeath et al. 2016). Open clusters (OCs), gravitationally bound systems of tens to thousands of stars, are the rare survivors of the embedded clusters gestated in molecular clouds (Elmegreen & Clemens 1985; Bastian & Goodwin 2006), with ages spanning a broad range from a few million years (Myr) to tens of billions of years. At present, the formation, evolution, and eventual dispersal of OCs are still poorly understood (e.g., Proszkow et al. 2009; Farias et al. 2018; Hao et al. 2023), although thousands of Galactic OCs have been discovered (e.g., Hao et al. 2022b; Castro-Ginard et al. 2022; Hunt & Reffert 2023). In order to better understand the formation and evolution of OCs, one of the key aspects is to obtain a detailed characterization of their internal kinematics (see Della Croce et al. 2023, and references therein). Hydrodynamical simulations of the cluster formation and very early evolution suggest that rotation may be common in the progenitors of OCs (e.g., Mapelli 2017). However, unlike the Galactic globular clusters, whose rotation has been studied extensively (e.g., van Leeuwen et al. 2000; Lanzoni et al. 2018; Leanza et al. 2022), our knowledge about the internal rotation of OCs is sorely lacking.

To date, the signals of rotation have been reported in only about a dozen of OCs. By identifying the correlation between the tangential velocities and the parallaxes of member stars, Vereshchagin & Chupina (2013) and Vereshchagin et al. (2013) explored the potential rotation in the Hyades and Pleiades clusters, and speculated that their rotation was comparable. Similarly, Kamann et al. (2019) and Healy et al. (2021) studied the tangential or radial velocities of cluster members as a function of distances to the cluster center, and they reported the presence of rotational signals

in the Praesepe and NGC 6791 and the absence of rotational signals in the Pleiades and NGC 6819. Based on the second data release of *Gaia* (DR2, Gaia Collaboration et al. 2016; Gaia Collaboration et al. 2018), Loktin & Popov (2020) analyzed the rotation in the Praesepe through the residual proper motion or radial velocity methods. Recently, by using the early data release 3 of *Gaia* (EDR3, Gaia Collaboration et al. 2021) to perform vector-field inference and create spatio-kinematic maps of OCs, Guilherme-Garcia et al. (2023) reported the detection of rotation patterns in eight clusters, with nine additional objects displaying possible rotation signs. However, all these studies adopted the methods of projection motion (proper motion or radial velocity) to study the rotation of OCs. The three-dimensional (3D) rotation of OCs, especially their rotation nature, remained elusive until the 3D rotation of Praesepe was revealed by Hao et al. (2022a, hereafter, Paper I).

Observationally, studying the 3D rotation of OCs is challenging. One of the main difficulties is obtaining a detailed characterization of the internal stellar kinematics, which requires high-quality measurements of the proper motions and radial velocities for the member stars. For the OCs with dozens to hundreds of members assembled in crowded fields, the precise spatial positions, and especially, the parallaxes of the member stars, are additional difficulties when rotation is to be inferred. *Gaia* DR3 (Gaia Collaboration et al. 2023) opens the possibility of new studies of stellar cluster dynamics. Considering the data quality of *Gaia* DR3, we focus on the nearby OCs that are rich in member stars, as *Gaia* DR3 is able to provide high-precision astrometric parameters and especially the radial velocities for a sufficient number of their member stars. In addition, reliable membership determination of an OC is also critical for revealing its internal rotation. After cross-matching a series of large-scale surveys to complement the *Gaia* catalog, Lodieu et al. (2019a,b) provided revised membership lists of four nearby star-rich OCs based on comprehensive analyses, including the Pleiades, Praesepe, Alpha Persei (α Per), and the Hyades. The ages of these four OCs span tens to hundreds of million years. In Paper I, we have developed the data-analyzing method and studied the Praesepe. In this work, we aim to assess the 3D rotation of the Pleiades, α Per, and the Hyades with *Gaia* DR3, and then explore the possible relation between the rotation of OCs and the cluster parameters (e.g., age, mass, and radius).

The Pleiades, also known as the Seven Sisters, are easily visible to the naked eye in the constellation of Taurus (Lynga 1981). The distance to the Pleiades has been estimated by many methods, such as the trigonometric parallax (e.g., Gatewood et al. 2000; Soderblom et al. 2005), fitting a color-magnitude diagram (e.g., An et al. 2007), and adoption of the eclipsing binaries as standard candles (e.g., Southworth et al. 2005). Currently, the distance to the Pleiades has been agreed to be the mean value of 130–140 pc (Melis et al. 2014; Gaia Collaboration et al. 2016). The age of the Pleiades cluster is a subject of debate, with estimates ranging from 70 to 80 Myr based on comparisons of the color-magnitude diagram of the cluster with theoretical isochrones of stellar evolution (e.g., Mermilliod 1981; Vandenberg & Bridges 1984), to 120–130 Myr derived from the lithium-depletion boundary method (e.g., Basri et al. 1996; Dahm 2015), and 132 Myr inferred from the white dwarf in the cluster (Lodieu et al. 2019a). In addition, the Pleiades contain more than 1000 member stars that share common proper motions of $(\mu_{\alpha^*}, \mu_{\delta}) \sim (19.5, -45.5)$ mas yr⁻¹, a high Galactic latitude ($b \sim 24^\circ$), and low reddening along the line of sight of $E(B - V) = 0.03$ mag (see Jones 1981; Robichon et al. 1999; van Leeuwen 2009). This cluster has a tidal radius of 11.6–19.5 pc, a core radius of 0.9–3.0 pc, and a cluster mass of 721–870 M_⊙ (Pinfield et al. 1998; Raboud & Mermilliod 1998; Converse & Stahler 2008, 2010).

The cluster α Per, also known as Melotte 20 or Collinder 39 (Melotte 1915; Collinder 1931), is located in the northern constellation of Perseus. It is composed of several blue B-type stars (Zuckerman et al. 2012). The distance to this cluster is estimated to be between 170 and 190 pc (Robichon et al. 1999; van Leeuwen 2009; Majaess et al. 2011; Gaia Collaboration et al. 2018). The trigonometric parallax and infrared color-magnitude diagram fitting methods give consistent distances for α Per, making it a benchmark on the cosmic distance ladder. In a comprehensive study, Lodieu et al. (2019a) derived a mean distance of 177.7 ± 0.8 pc for the cluster. Furthermore, the α Per has an estimated age of approximately 50–70 Myr (Prosser et al. 1996; Makarov 2006). Its extinction along the line of sight is estimated to be $A_V = 0.30$ mag, with a possible differential extinction (Prosser 1992). The α Per is located at a low Galactic latitude of ($b \sim -7^\circ$, e.g., Makarov 2006; van Leeuwen 2009), has a proper motion of $(\mu_{\alpha^*}, \mu_{\delta}) \sim (23.1, -25.8)$ mas yr⁻¹ (Lodieu et al. 2019a), a core radius of 2.3 ± 0.3 pc, and a tidal radius of ~ 9.5 pc (Lodieu et al. 2019a).

The Hyades, regarded as a sister cluster of the Pleiades, is the nearest open cluster and one of the best-studied star clusters (Messier 1781). Using the *Hipparcos* dataset, Perryman et al. (1998) deduced the cluster distance to be 46.3 ± 0.3 pc, similar to the results obtained by using the *Hubble* Space Telescope measurements (McArthur et al. 2011) and infrared color-magnitude diagram fitting (Majaess et al. 2011). Based on the *Gaia*'s trigonometric parallax, the distance of the cluster has been updated to 47.0 ± 0.2 pc (Lodieu et al. 2019a). The age of the Hyades cluster has been estimated by different methods, such as the theoretical isochrone fitting method (625 ± 50 Myr, Maeder

& Mermilliod 1981; Mermilliod 1981), the cooling age of white dwarf members (648 ± 45 Myr, De Gennaro et al. 2009), and the method of the lithium-depletion boundary (650 ± 70 Myr, Lodieu et al. 2018). The cluster consists of a roughly spherical group of hundreds of member stars presenting the proper motions of 70–140 mas yr⁻¹ on the sky (Perryman et al. 1998; van Leeuwen 2009; Lodieu et al. 2019a). The cluster has a core radius of 2.5–3.0 pc and a tidal radius of 10 pc (see Perryman et al. 1998; Röser et al. 2011). The reddening of the Hyades is low, with $E(B - V) \leq 0.001$ mag (Taylor 2006).

With the high-quality data from *Gaia* DR3, the focus of this work is to reveal the internal kinematics of the Pleiades, α Per, and the Hyades clusters in detail. We first update the catalog of member stars of the three OCs based on *Gaia* DR3, and then we extract those members with astrometric parameters and radial velocities. Subsequently, we update the method used in Paper I to investigate the rotation of the Pleiades, α Per, and the Hyades. When a cluster does rotate, we determine its rotation axis, derive the rotational velocities, and analyze the rotational characteristics of the member stars. Finally, we discuss the possible relations between the internal rotation of OCs and the cluster parameters.

2. DATA

To study the internal kinematics of OCs, we adopt the *Gaia* DR3 dataset. The astrometric and photometric parameters in *Gaia* DR3 are inherited from *Gaia* EDR3, which contains celestial positions (R.A., Decl.), parallaxes (ϖ), proper motions (μ_{α^*} , μ_{δ}), and three photometric passbands (G , G_{BP} , and G_{RP}) of more than a billion stellar sources. In addition, in comparison to *Gaia* DR2, more than 33 million objects with new determinations of the mean radial velocities are also included in *Gaia* DR3. In this work, we adopt the radial velocity measurements provided by *Gaia* DR3 to ensure the sample homogeneity and avoid the potentially large systematic errors.

Table 1. Number of the member stars selected in different (sub) samples or different steps for the Pleiades, α Per, and the Hyades.

	Pleiades	α Per	Hyades
Initial sample ^a	2281	3162	1764
Step 1	66	182	87
Step 2	75	256	133
Step 3	77	894	907
Step 4	265	596	45
Sample ^b	1798	1234	592
Step 5	226	137	215
Step 6	1	0	1
Subsample ^c	225	137	214

NOTE—For details of Steps 1–6 see Section 2.

^aThe membership lists are from Lodieu et al. (2019a) for the Pleiades and α Per, and from Lodieu et al. (2019b) for the Hyades.

^bAfter subtracting the member stars processed in “Steps 1–4” from the “Initial sample”, the samples contain the stars with reliable astrometric parameters provided by *Gaia* DR3.

^cAfter subtracting the member stars processed in “Step 6” from those of “Step 5”, the subsamples contain the stars with radial velocities provided by *Gaia* DR3.

The Pleiades, α Per, and the Hyades are three member-rich OCs in the solar neighborhood that span a wide range of ages. We initiate the study by adopting the membership lists of the Pleiades, Hyades, and α Per clusters provided by Lodieu et al. (2019a,b). Lodieu et al. (2019a) combined the *Gaia* DR2 dataset with multiple large-scale public surveys from the optical to mid-infrared wavelengths to provide the revised membership lists for the Pleiades and α Per clusters. The selection criteria for the member stars in Lodieu et al. (2019a) are initially designed to be as inclusive as possible and become more selective in the later process. Finally, they obtained 2281 member stars for the Pleiades and 3162 member stars for the α Per. With the same method, Lodieu et al. (2019b) compiled a list of member stars

for the Hyades cluster, which includes a total of 1764 member stars. We use *Gaia* DR3 to update the aforementioned three membership lists. The details are described below. The numbers of selected member stars in each step are given in Table 1.

- Step 1. Selection of the unmatched members after cross-matching the member stars with the *Gaia* DR3 database through *Gaia*'s `source_id`.
- Step 2. Removal of the members that lack astrometric (ϖ , μ_{α^*} , μ_{δ}) or photometric (G , G_{BP} , and G_{RP}) parameters.
- Step 3. Rejection of those members that lie beyond three times of the tidal radius (r_{td}) from the cluster center. The distances of the members to the cluster center are taken from Lodieu et al. (2019a,b).
- Step 4. Selection of the members that have large parallax and/or proper motion uncertainties based on the exclusion criteria of the typical uncertainties of the faint stars ($G = 20$) observed by *Gaia*, i.e., $e_{\varpi} \geq 0.5$ mas, and $e_{\mu_{\alpha^*}, \delta} \geq 0.6$ mas yr $^{-1}$ (Gaia Collaboration et al. 2023). Member stars whose parallaxes and/or proper motions significantly deviate (three times the standard deviation) from the overall sample are also excluded.
- Step 5. Selection of the members with radial velocity measurements and corresponding uncertainties smaller than 2 km s $^{-1}$, which is the same as Paper I. Members whose radial velocities significantly deviate from the overall sample are also deleted.
- Step 6. Elimination of the nonsingle members that have not been correctly handled in the *Gaia*'s astrometric solution according to the criterion of `ipd_gof_harmonic_amplitude` > 0.1 and `ruwe` > 1.4 (Gaia Collaboration et al. 2021).

3. METHODS

The basic steps we develop to study the 3D rotation of OCs are described in detail in Paper I. Here, we only give a brief description. First, we use the astrometric parameters of the cluster members to determine their coordinates (x_g , y_g , z_g) and velocities (v_{x_g} , v_{y_g} , v_{z_g}) in the Galactic Cartesian coordinate system (O_g - $X_gY_gZ_g$), where the uncertainties are estimated with a Monte Carlo method by taking into account the observational errors. Second, the coordinates (x_c , y_c , z_c) and velocities (v_{x_c} , v_{y_c} , v_{z_c}) of the members in the cluster Cartesian coordinate system (O_c - $X_cY_cZ_c$) are converted from those in the O_g - $X_gY_gZ_g$ system. Third, based on the velocities (v_{x_c} , v_{y_c} , v_{z_c}) of the cluster members, we calculate the 3D mean residual velocities and estimate their uncertainties with Monte Carlo simulations in order to investigate their dependence on the position angles (PA; i.e., α , β , and γ in Figure A1), as well as to check the rotation of the cluster and determine the rotation axis \vec{l} . Afterward, the coordinates (x_r , y_r , z_r) and velocities (v_{x_r} , v_{y_r} , v_{z_r}) of the members in the cluster rotation Cartesian coordinate system (O_r - $X_rY_rZ_r$, Figure A1) can be obtained according to the rotation axis, which can then be transformed into the cylindrical coordinate system (r , φ , z) to reveal the internal rotation of an OC.

Based on the above steps, we have made some updates in this work. First, the method is improved by analyzing the mean residual velocity of member stars within three times, one time, and half of the cluster's tidal radius (r_{td}) as a function of PAs, respectively. This approach can enhance the reliability of the rotation representation within the cluster and better determine the rotation axis \vec{l} . Another improvement addresses the difficulty of determining the cluster rotation axis in the O_c - $X_cY_cZ_c$ system when the rotational signals (sinusoidal behavior) are not significant in all three dimensions simultaneously. To fix this problem, we rotate the O_c - $X_cY_cZ_c$ system around its origin (O_c) with a given angle. Concretely speaking, with a set of PAs (α_0 , β_0 , γ_0), we transform the 3D coordinates and velocity components of cluster members from the O_c - $X_cY_cZ_c$ system into the rotated Cartesian coordinate system (signed as O'_r - $X'_rY'_rZ'_r$). Subsequently, we use the residual velocity method to determine the rotation in the cluster and estimate the PAs (α' , β' , γ') of the rotation axis \vec{l} in the rotated system. Then, the vectors of the rotation axis \vec{l} can be converted from the O'_r - $X'_rY'_rZ'_r$ system back into the O_c - $X_cY_cZ_c$ system via

$$\begin{pmatrix} x_c \\ y_c \\ z_c \end{pmatrix} = \begin{pmatrix} \cos \alpha_1 & \cos \alpha_2 & \cos \alpha_3 \\ \cos \beta_1 & \cos \beta_2 & \cos \beta_3 \\ \cos \gamma_1 & \cos \gamma_2 & \cos \gamma_3 \end{pmatrix} \begin{pmatrix} x_r \\ y_r \\ z_r \end{pmatrix}, \quad (1)$$

where α_i , β_i , and γ_i are the included angles between the axes of the $O_c-X_cY_cZ_c$ system and those of the $O'_r-X_rY_rZ_r$ system. When the vectors of \vec{l} in the $O_c-X_cY_cZ_c$ system are obtained, the PAs of \vec{l} in the $O_c-X_cY_cZ_c$ system (α , β , γ) can be determined. Then, we continue to perform the aforementioned procedures to analyze the internal rotation of an OC.

In the same way as in Paper I, to elucidate the rotational nature of the member stars of an OC, we compare their root-mean-square (RMS) rotational velocities and the theoretical predictions from Newton's theorems, with the following equation:

$$v_c(r) = \left[GM_t \cdot \frac{r^2}{(r^2 + r_{co}^2)^{3/2}} \right]^{1/2}. \quad (2)$$

Here, $G = 4.3 \times 10^{-3} \text{ pc M}_\odot^{-1} (\text{km s}^{-1})^2$ is the gravitational constant, r_{co} is the core radius, and M_t is the cluster mass inside the tidal radius.

4. RESULTS

4.1. Rotation in Praesepe with Gaia DR3

In Paper I, we studied the rotational properties of the Praesepe cluster based on *Gaia* EDR3. In comparison to EDR3, *Gaia* DR3 provides high-precision radial velocity measurements for more cluster members. We reanalyze the Praesepe rotation with the new data of cluster members and the amended method described above. We find that the features of the mean residual velocities of the member stars within $3 r_{td}$, $1 r_{td}$, and $0.5 r_{td}$ of the Praesepe all confirm the 3D rotation in the cluster. In addition, the rotational characteristics of member stars within the cluster tidal radius are almost consistent with those in Paper I and can be well described by Newton's theorems. Moreover, the new dataset still shows no expansion or contraction in the Praesepe. As shown in Table 2, by comparison, the consistent parameters confirm that the results obtained in Paper I are reliable, and the new data-analyzing method updated in this work is feasible.

Table 2. Comparison of the rotational parameters of the Praesepe for the results obtained in this work and those in Paper I.

	This work	Paper I
Position angles	α, β, γ	α, β, γ
0.5 r_{td}	$119^\circ \pm 10^\circ, 133^\circ \pm 12^\circ, 214^\circ \pm 8^\circ$	–
1.0 r_{td}	$128^\circ \pm 4^\circ, 132^\circ \pm 7^\circ, 212^\circ \pm 5^\circ$	$121^\circ \pm 5^\circ, 118^\circ \pm 17^\circ, 211^\circ \pm 8^\circ$
3.0 r_{td}	$136^\circ \pm 6^\circ, 148^\circ \pm 5^\circ, 210^\circ \pm 5^\circ$	$140^\circ \pm 3^\circ, 152^\circ \pm 7^\circ, 210^\circ \pm 2^\circ$
\vec{l} vs. GP	$34^\circ \pm 15^\circ$	$41^\circ \pm 12^\circ$
Rotation velocity	$0.12 \pm 0.05 \text{ km s}^{-1}$	$0.16 \pm 0.05 \text{ km s}^{-1}$
Core radius	$2.0 \pm 0.4 \text{ pc}$	$1.6 \pm 0.5 \text{ pc}$
Tidal mass	$609 \pm 135 \text{ M}_\odot$	$537 \pm 146 \text{ M}_\odot$

NOTE— r_{td} : tidal radius of the Praesepe. GP: Galactic plane. \vec{l} vs. GP: the included angle between \vec{l} and the Galactic plane.

4.2. The Pleiades cluster

Figure 1 shows the multidimensional distributions of astrometric parameters (R.A., Decl., ϖ , μ_{α^*} , μ_δ) and color-magnitude diagram of all the member stars (grey) and those with radial velocities (red) for the Pleiades. The observed parameters of the member stars can be approximated by a multidimensional normal distribution. In this section, we describe the rotational properties of the Pleiades cluster and explore the rotational characteristics of the cluster members.

4.2.1. Rotation in the Pleiades

For the 225 member stars with radial velocities (see Table 1), the median uncertainties of parallax, proper motion μ_{α^*} and μ_δ are 0.02 mas, 0.02 mas yr $^{-1}$, and 0.02 mas yr $^{-1}$, respectively. The median uncertainty of radial velocity is 0.6 km s $^{-1}$. Based on these member stars, the means and standard deviations of the astrometric parameters

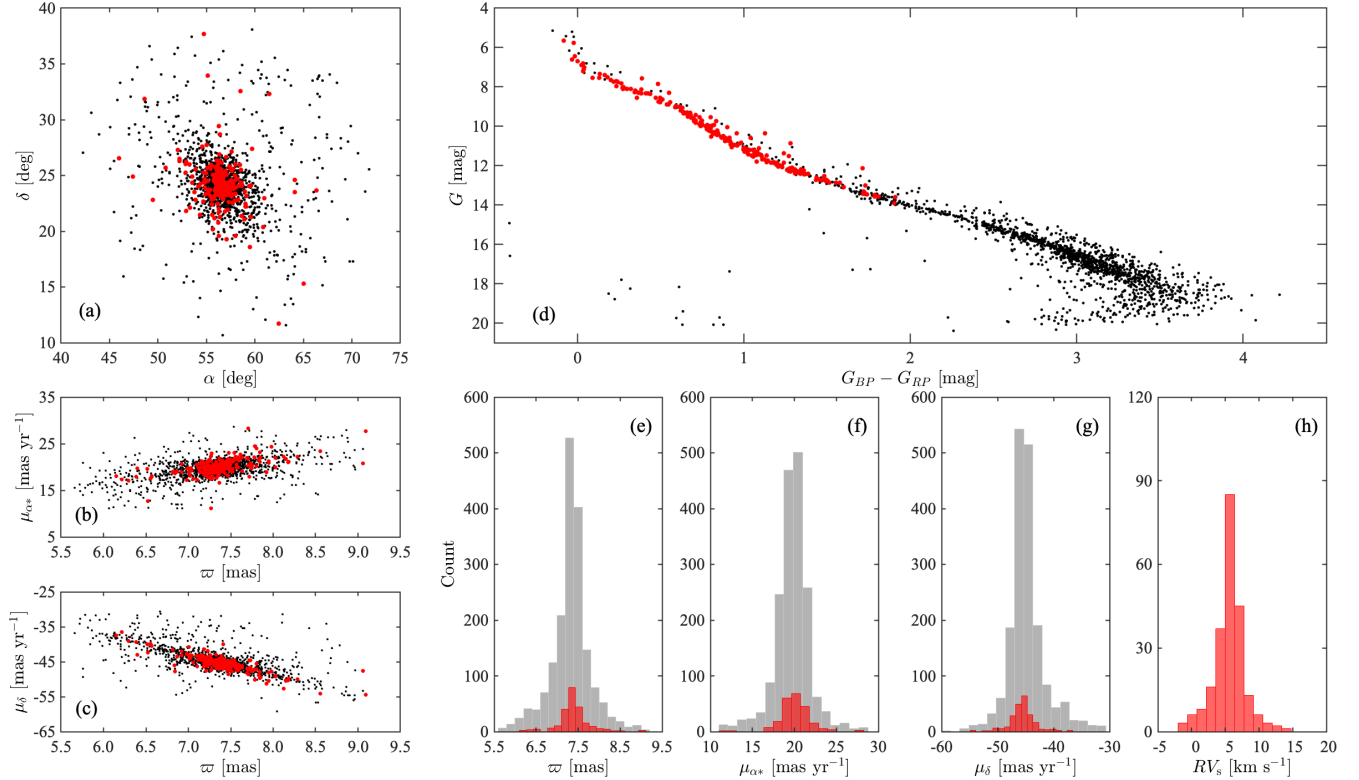


Figure 1. Multidimensional distributions of all the member stars (gray) and those with radial velocity measurements (red) for the Pleiades cluster. Panel (a): the distribution in the sky; Panels (b) and (c): the relationship between parallax and proper motions; Panel (d): the color-magnitude diagram; Panels (e), (f), (g) and (h): the histograms of parallax, proper motions and radial velocity, respectively.

of the Pleiades cluster are determined as: (R.A., Decl.) = $(56.58^\circ \pm 2.51^\circ, 24.35^\circ \pm 2.47^\circ)$, $\varpi = 7.38 \pm 0.37$ mas, proper motions $(\mu_{\alpha^*}, \mu_\delta) = (20.04 \pm 1.80, -45.40 \pm 2.59)$ mas yr $^{-1}$, and radial velocity $RV = 5.57 \pm 0.77$ km s $^{-1}$. These values are consistent with the previous determinations (Liu et al. 1991; Mermilliod et al. 1997; Gao 2019; Gaia Collaboration et al. 2018; Lodieu et al. 2019a). With these parameters, we derive the 3D coordinates and velocities of the Pleiades and its member stars in the Galactic Cartesian coordinate system ($O_g-X_gY_gZ_g$), and then transform them to the $O_c-X_cY_cZ_c$ system. After that, the mean residual velocities and uncertainties of the member stars as a function of PAs are calculated. We assign an r_{td} of 11.6 pc to the Pleiades cluster, which comes from Lodieu et al. (2019a). Figure 2 (a–c), (d–f), and (g–i) present the mean residual velocities as functions of PAs for the member stars within $3 r_{td}$, $1 r_{td}$, and $0.5 r_{td}$, respectively. The error bars in the figures are the uncertainties of the mean residual velocities. As shown in Figure 2, the clear sinusoidal behaviors indicate the presence of 3D rotation in the Pleiades cluster.

Table 3. Best-fit PAs of the Pleiades cluster.

	α	β	γ
$3.0 r_{td}$	$81^\circ \pm 4^\circ$	$78^\circ \pm 7^\circ$	$295^\circ \pm 7^\circ$
$1.0 r_{td}$	$102^\circ \pm 8^\circ$	$59^\circ \pm 11^\circ$	$337^\circ \pm 7^\circ$
$0.5 r_{td}$	$100^\circ \pm 7^\circ$	$54^\circ \pm 10^\circ$	$337^\circ \pm 10^\circ$

NOTE— r_{td} : tidal radius of the Pleiades.

Using the residual velocity method, the PAs (α, β, γ) of the rotation axis \vec{l} of the Pleiades cluster in the $O_c-X_cY_cZ_c$ system can be determined. The best-fitting results are shown in Table 3 and Figure 2, where the errors come from

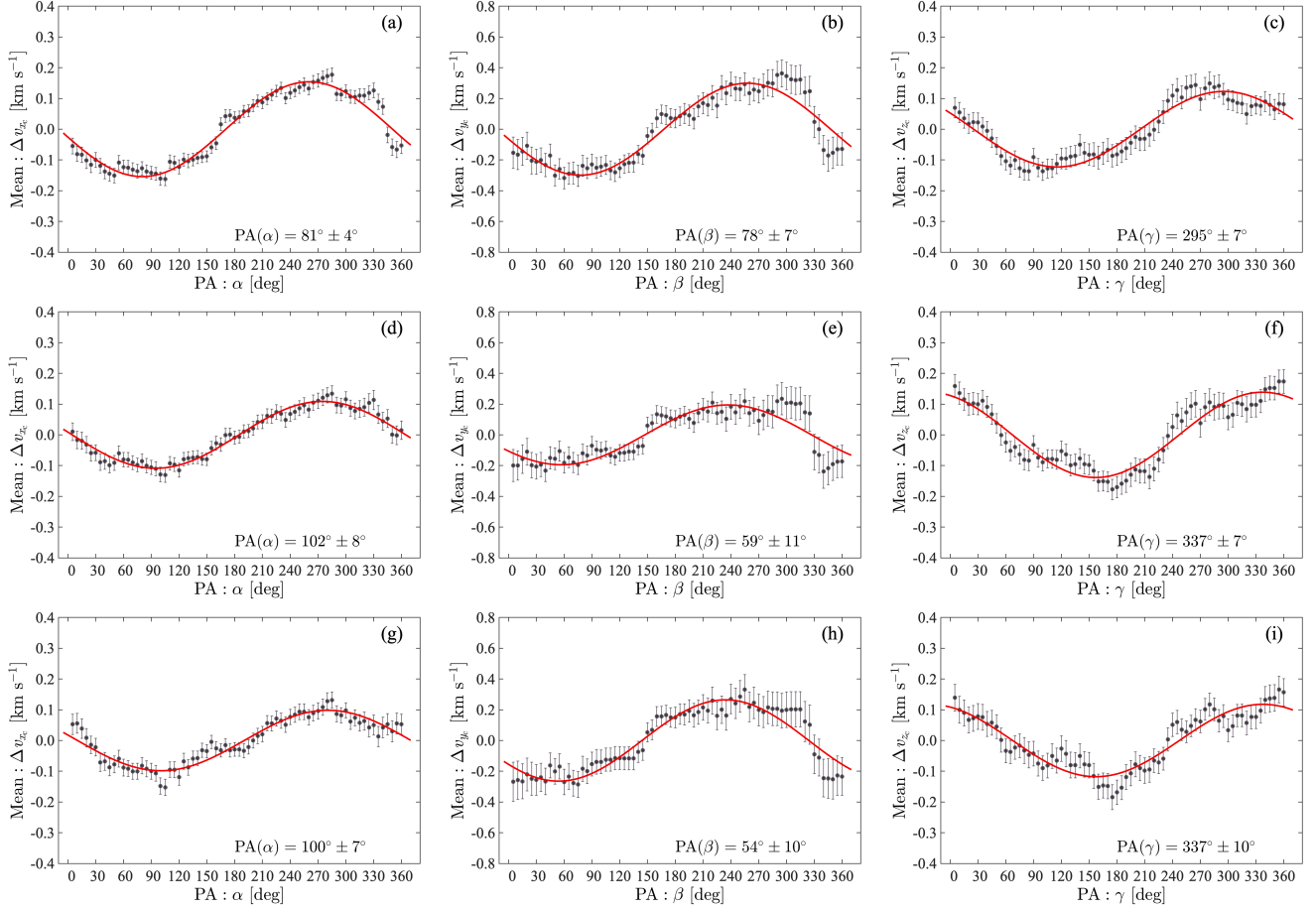


Figure 2. Mean residual velocities as a function of the position angles (PAs) for the Pleiades. The left, middle, and right panels show the v_{x_c} vs. α , v_{y_c} vs. β , and v_{z_c} vs. γ plots, respectively. The results for the member stars within three times of the tidal radius (Panels a, b, c), within a tidal radius (Panels d, e, f), and within half a tidal radius (Panels g, h, i) are shown from top to bottom, respectively. The error bars (gray) and the best-fitting sine function (red) are also shown in each panel.

the Monte Carlo simulations by considering the uncertainties of the mean residual velocities. The PAs obtained by the member stars within $1 r_{td}$ are consistent with those fitted by using the members within $0.5 r_{td}$. They satisfy the relation of $\tan \alpha \cdot \tan \gamma = \tan \beta$ considering the uncertainties. Nevertheless, the PAs obtained by the member stars of the entire sample are different from the above results, although the three angles also satisfy $\tan \alpha \cdot \tan \gamma = \tan \beta$ considering the uncertainties. This phenomenon aligns with the findings in Paper I for the Praesepe cluster, which may be due to the fact that the member stars located outside the cluster’s tidal radius are not only dominated by the OC itself, but also by the tidal force of the Milky Way.

We employ the best-fitting PAs for the member stars within $1 r_{td}$ to determine the rotation axis \vec{l} of the Pleiades cluster. The angle between \vec{l} and the Galactic plane is estimated to be $62^\circ \pm 13^\circ$, where the errors come from the uncertainties of the obtained PAs. Considering the relationship of $\tan \alpha \cdot \tan \gamma = \tan \beta$, we adopt $(\alpha, \beta, \gamma) = (102^\circ, 63^\circ, 337^\circ)$ to derive the vectors of the X_r , Y_r , and Z_r axes in the $O_c-X_cY_cZ_c$ system, as described in Section 3. Then, the 3D coordinates and velocity components of the member stars are transformed from the $O_c-X_cY_cZ_c$ system to the $O_r-X_rY_rZ_r$ system, and eventually converted to the 3D coordinates (r, φ, z) and velocity components (v_r, v_φ, v_z) in the cylindrical coordinate system. Based on the rotational velocities (v_φ) and the corresponding uncertainties of the member stars within $1 r_{td}$, the mean rotation velocity of the Pleiades cluster is estimated to be 0.24 ± 0.04 km s⁻¹, which is in general agreement with the results illustrated in Figure 2.

4.2.2. Rotational properties of the member stars of Pleiades

Figure 3 presents the rotational velocities of the member stars of the Pleiades as a function of their distances from the cluster center. Within the tidal radius of the Pleiades (11.6 pc), the rotation velocities of the member stars in the

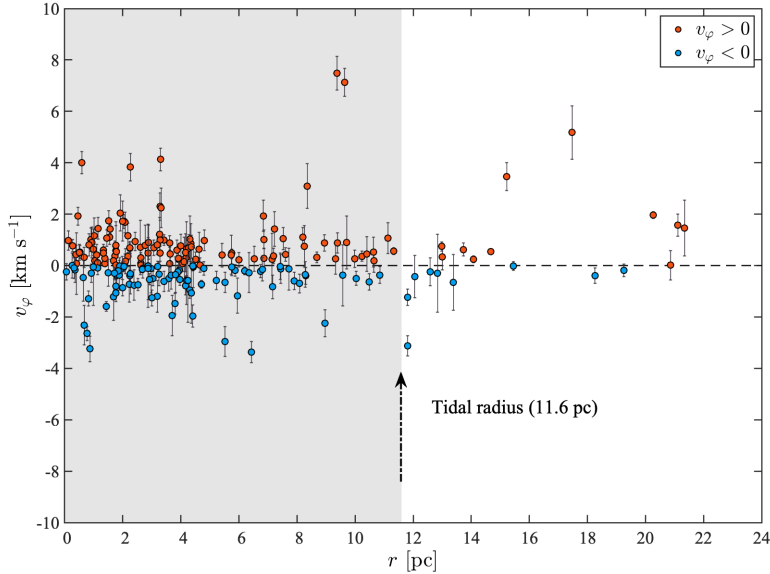


Figure 3. Rotational velocity as a function of the distance to the cluster center for the member stars within twice the tidal radius of the Pleiades.

Table 4. RMS rotational velocities of the member stars within the tidal radius of the Pleiades.

R_i [pc]	R_o [pc]	R_m [pc]	N	RMS v_ϕ [km s $^{-1}$]	$\epsilon_{\text{RMS } v_\phi}$ [km s $^{-1}$]
(1)	(2)	(3)	(4)	(5)	(6)
0.0	2.0	1.2	54	0.79	0.06
2.0	4.0	3.0	56	0.86	0.06
4.0	6.0	4.7	34	0.70	0.10
6.0	8.0	7.1	18	0.73	0.11
8.0	10.0	8.9	12	0.66	0.12
10.0	11.6	10.6	9	0.57	0.13

NOTE—Columns 1–2: the inner and outer distances of each bin; Columns 3–6: the average distance, the number of the member stars, RMS rotational velocity, and its uncertainty derived from the stars in each bin.

inner region are slightly higher than those in the outer region. Similar to the Presepe cluster (Paper I) and globular clusters (e.g., Lanzoni et al. 2018; Leanza et al. 2022), not all member stars rotate in the same direction. There are ~ 1.3 times as many member stars with positive rotational velocities as rotate with negative rotational velocities. This situation may be attributed to the presence of mutual interference of stellar feedback during the formation of the cluster progenitor. In Figure 3, the rotation of the member stars located close to or outside the cluster’s tidal radius seem to be disorganized, possibly because these member stars are partially affected by the Galactic tidal force and are not purely governed by the gravitational force of the cluster itself. In addition, within the tidal radius of the Pleiades, several stars exhibit peculiar rotational velocities that deviate from most of the cluster members, which may be passing stars and not the genuine members of the Pleiades.

We compare the observations with the theoretical predictions to address whether Newton’s theorems can describe the rotation of the member stars within the tidal radius of the Pleiades cluster. Firstly, we calculate the skewness of the astrometric parameters of the member stars within r_{td} to investigate the symmetry of their density distributions. The skewness of the Galactic longitude, Galactic latitude, and parallax are 0.1, -0.2 and 0.1, respectively, which confirms the assumption of a spherically symmetric distribution of the stars in the Pleiades. Further, we attempt to make a comparison between the RMS rotational velocities derived from the cluster members and the theoretical expectations of Newton’s theorems.

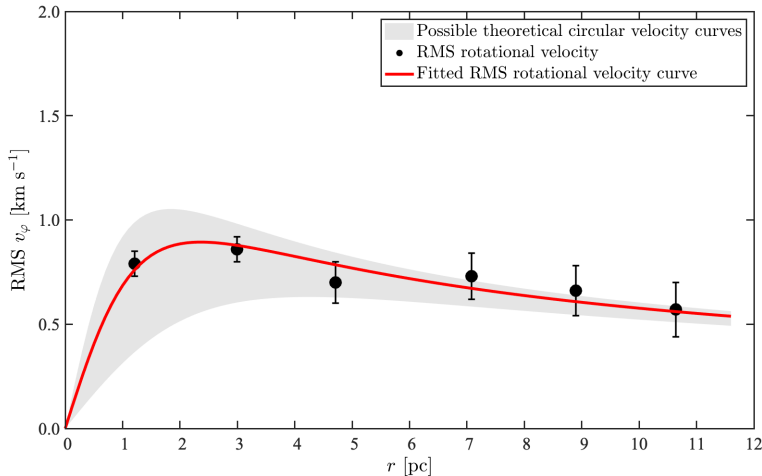


Figure 4. RMS rotational velocity as the function of distance to the center of the Pleiades cluster. The black dots denote the observed RMS rotational velocities of the member stars. The uncertainties are indicated by the error bars. The gray shadowed area shows the theoretical values calculated by Equation (2) after considering the possible ranges of the tidal mass and the core radius of the Pleiades. The red line is the best-fitting curve for the observed RMS rotational velocities.

For the 196 member stars within the tidal radius of the Pleiades cluster, the median absolute value of rotational velocities v_ϕ is $\sim 0.5 \text{ km s}^{-1}$, and the standard deviation is $\sim 1.0 \text{ km s}^{-1}$. To study the rotational characteristics displayed by the member stars of the Pleiades, we divide them into several bins based on their distances from the cluster center. A few stars have peculiar rotational velocities that significantly deviate from those of most member stars. We identify 13 such kind of stars by checking the distribution of the rotational velocities of the member stars in each bin and eliminate them. Then, we compute the RMS rotation velocity in each distance bin and estimate the corresponding uncertainties using the Monte Carlo simulations. The results are presented in Table 4 and Figure 4.

With Equation (2), the theoretical rotational velocity profile provides a good fit to the RMS rotation velocities of the cluster members. In addition, based on previous estimates of the tidal mass and core radius (see Section 1), we calculate the possible theoretical circular velocity curves for the Pleiades cluster, as shown by the gray shaded area in Figure 4. It is clear that the best-fit RMS rotational velocity curve is consistent with the theoretical predictions. Therefore, we argue that Newton’s theorems is capable of characterizing the rotational properties of the member stars within the tidal radius of Pleiades. Based on the result in Table 4 and Equation (2), we estimate the core radius and the mass within r_{td} to be $1.7 \pm 0.3 \text{ pc}$ and $806 \pm 144 M_\odot$, respectively, where the errors are estimated with the Monte Carlo simulations. These two values agree well with previous results (see Section 1).

The Pleiades are about 100 Myr old (see Section 1). Whether the Pleiades cluster is expanding or contracting can be examined by a statistical analysis of the radial components v_r of the member stars perpendicular to the cluster rotation axis. In Figure 5, the mean radial components \bar{v}_r of the member stars within $0.5 r_{\text{td}}$, $1 r_{\text{td}}$, and $3 r_{\text{td}}$ are $0.0 \pm 0.05 \text{ km s}^{-1}$, $0.1 \pm 0.04 \text{ km s}^{-1}$, and $-0.1 \pm 0.04 \text{ km s}^{-1}$, respectively. Here, the errors are obtained with the Monte Carlo method by taking into account the uncertainties of v_r . These results indicate the absence of expansion or contraction in the Pleiades cluster, and this implies that the rotation of the member stars within r_{td} can exhibit closed-loop motions. However, as shown in Figure 5, we note the presence of non-negligible radial component acceleration and dispersion of members in the Pleiades, although the dispersion is partially influenced by the astrometric measurement uncertainties. Considering the absence of expansion or contraction in the Pleiades, the system should possess additional mass to provide the force that support the radial components acceleration of the member stars. Hence, the derived mass of the Pleiades cluster represents a lower limit.

4.3. Cluster α Per

Similar to Figure 1, we present the multidimensional distributions and color-magnitude diagram for cluster α Per in Figure 6. In this section, we show the rotational properties of cluster α Per, and analyze the rotational characteristics of the cluster members.

4.3.1. Rotation in α Per

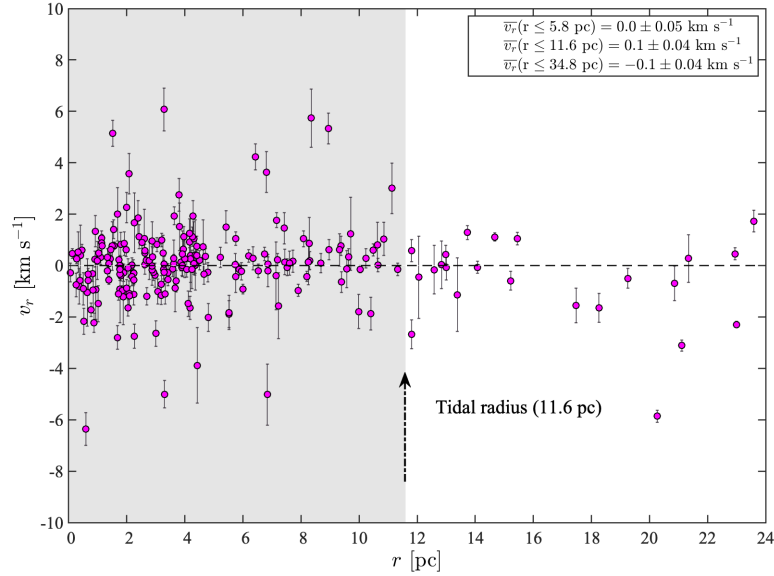


Figure 5. Radial velocity as a function of the distance to the cluster center, for the member stars of the Pleiades. The mean values of the radial components within $0.5 r_{\text{td}}$, $1 r_{\text{td}}$, and $3 r_{\text{td}}$ are close to zero, as shown in the panel.

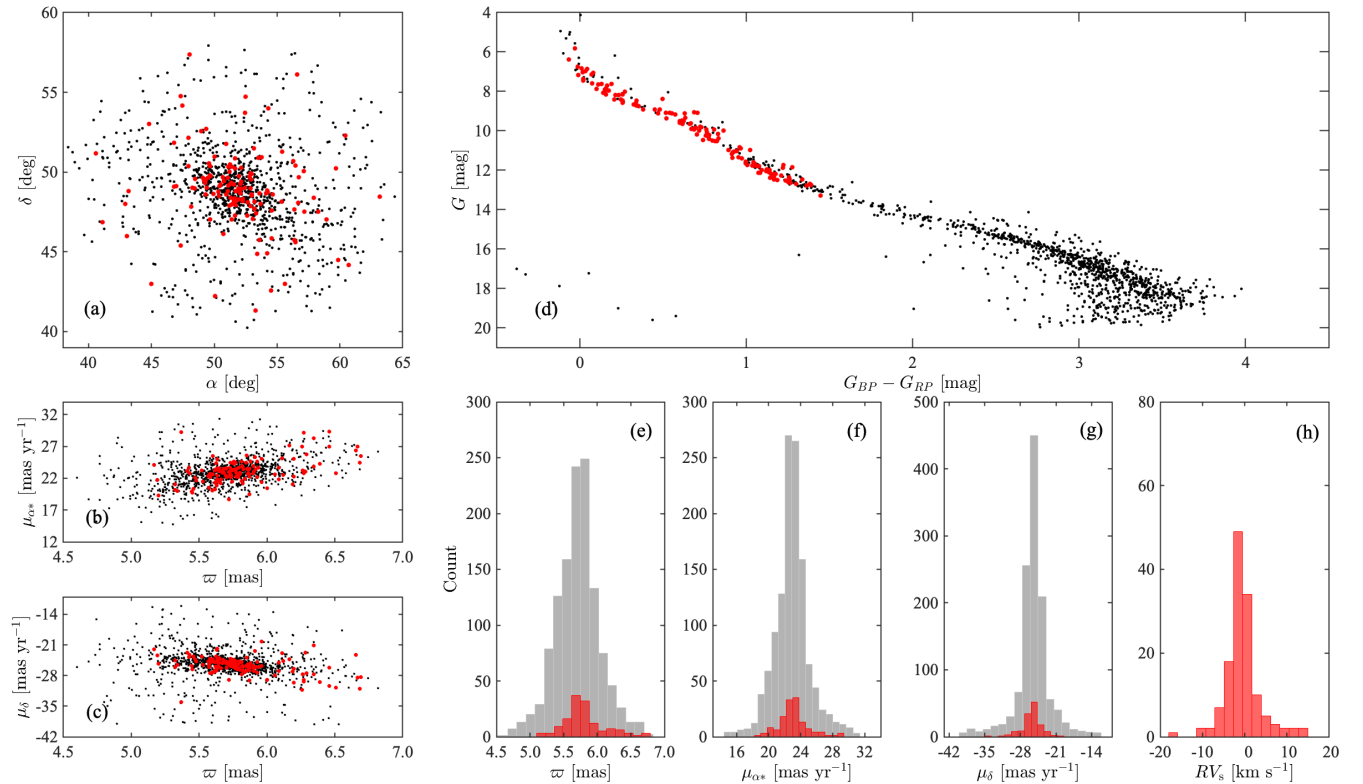


Figure 6. Same as Figure 1, but for the α Per cluster.

For the 137 member stars with radial velocities (see Table 1), the median uncertainties of the parallax, proper motion μ_{α^*} and μ_{δ} , and for the radial velocity are 0.02 mas , 0.02 mas yr^{-1} , 0.02 mas yr^{-1} , and 0.9 km s^{-1} , respectively. Based on the observational parameters of these member stars, the means and standard deviations of the fundamental

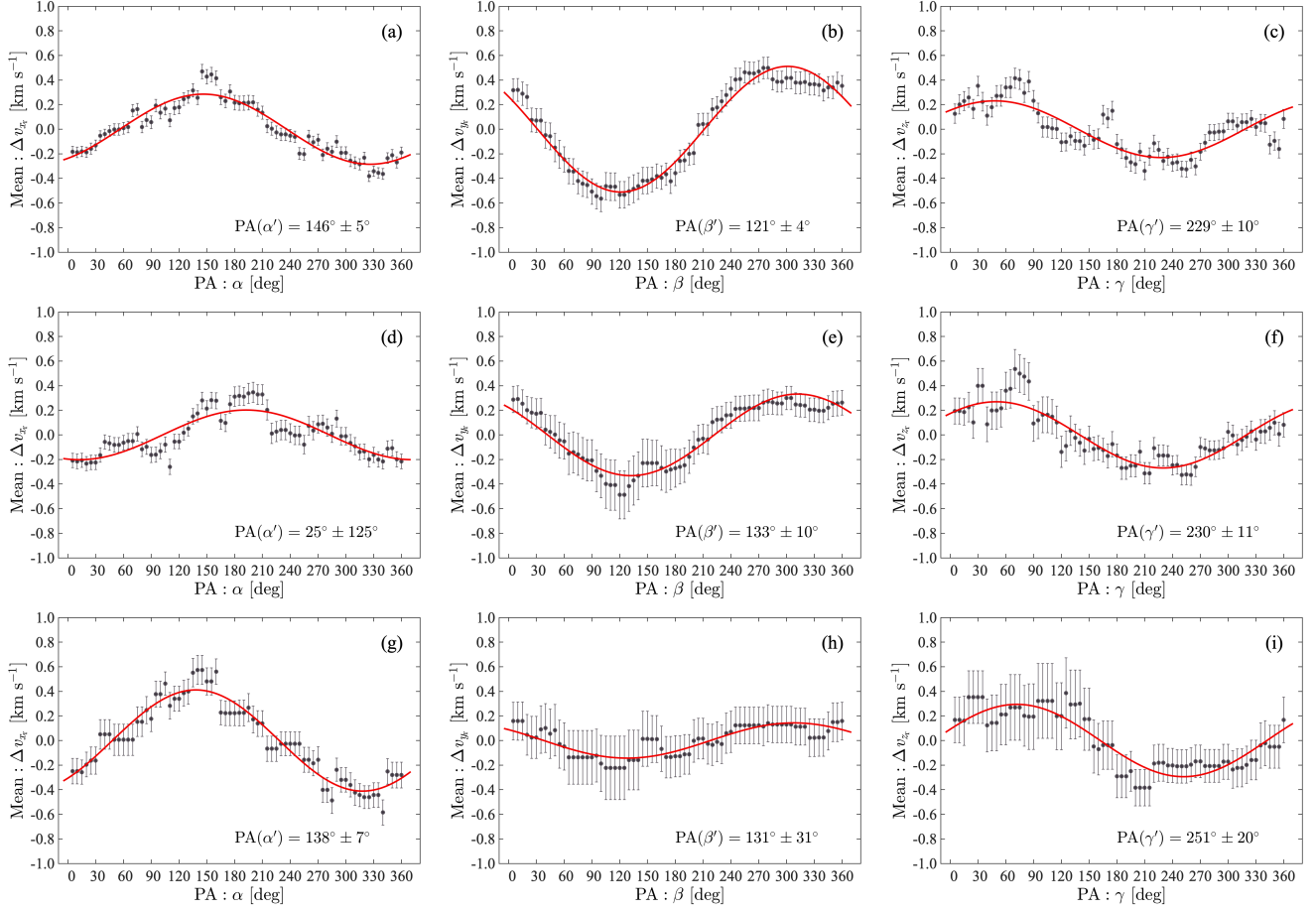


Figure 7. Same as Figure 2, but for the α Per cluster.

astrometric parameters of the α Per cluster are determined as: (R.A., Decl.)=($51.87^\circ \pm 3.65^\circ$, $48.93^\circ \pm 2.47^\circ$), $\varpi = 5.81 \pm 0.30$ mas, $(\mu_{\alpha^*}, \mu_{\delta}) = (23.11 \pm 1.87, -25.76 \pm 1.97)$ mas yr $^{-1}$, and $RV = -0.43 \pm 4.10$ km s $^{-1}$, which are in good agreement with previous determinations (Stauffer et al. 1989; Prosser 1994; Mermilliod et al. 2008; Gaia Collaboration et al. 2018; Lodieu et al. 2019a). Similar to the Pleiades, we obtain the 3D coordinates and motion of the α Per cluster in the $O_g-X_gY_gZ_g$ system and the 3D coordinates and motions of its member stars in the $O_c-X_cY_cZ_c$ system.

The direct usage of the residual velocity method in the $O_c-X_cY_cZ_c$ system captures the rotation signals of the α Per cluster, but does not allow a good determination of the PAs (α , β , γ) of the rotation axis \vec{l} . In order to resolve this matter, as described in Section 3, we rotate the $O_c-X_cY_cZ_c$ system around its origin with a set of angles $(\alpha_0, \beta_0, \gamma_0) = (40^\circ, 40^\circ, 45^\circ)$. The 3D coordinates and velocity components of the cluster members are then transformed from the $O_c-X_cY_cZ_c$ system to the rotated $O'_r-X_rY_rZ_r$ system. After this, in the same way as for the Pleiades, we estimate the residual velocities of the cluster members and uncertainties to determine the PAs (α' , β' , γ') of the rotation axis \vec{l} of the α Per in the rotated system. Figure 7 presents the mean residual velocities as functions of PAs (α' , β' , γ') for the member stars within $3 r_{td}$ (a-c), $1 r_{td}$ (d-f), and $0.5 r_{td}$ (g-i) of the α Per cluster, where $r_{td} = 9.5$ pc is taken from Lodieu et al. (2019a). The sinusoidal relations between the mean residual velocities and PAs indicate the 3D rotation of the α Per cluster, although the result in Figure 7(d) is not very significant.

The fitted PAs (α' , β' , γ') of the rotation axis \vec{l} of the α Per cluster in the rotated system are listed in Table 5 and marked in Figures 7. The PAs fitted by the members within $0.5 r_{td}$ satisfy the relation of $\tan \alpha' \cdot \tan \gamma' = \tan \beta'$ considering the uncertainties. The PA α' value cannot be well determined by the members within $1 r_{td}$, which suffer from large uncertainties. Alternatively, PA $\alpha' = 138^\circ$ can be determined from the $\tan \alpha' \cdot \tan \gamma' = \tan \beta'$ relation, combined with the well-fit β' and γ' values. In this way, the three PAs are compatible with those derived by the members within $0.5 r_{td}$, and they can therefore be used to determine the rotation axis \vec{l} . Compared with the Pleiades

Table 5. Best-fit PAs of the α Per cluster.

	α'	β'	γ'
$3.0 r_{\text{td}}$	$146^\circ \pm 5^\circ$	$121^\circ \pm 4^\circ$	$229^\circ \pm 10^\circ$
$1.0 r_{\text{td}}$	$25^\circ \pm 125^\circ$	$133^\circ \pm 10^\circ$	$230^\circ \pm 11^\circ$
$0.5 r_{\text{td}}$	$138^\circ \pm 7^\circ$	$131^\circ \pm 31^\circ$	$251^\circ \pm 20^\circ$

NOTE— r_{td} : tidal radius of the α Per cluster.

cluster, the stronger rotation of the α Per cluster makes the PAs obtained by using the member stars within $3 r_{\text{td}}$ almost consistent with the above results, considering the uncertainties.

The PAs obtained by using the members within $1 r_{\text{td}}$ are employed to determine the rotation axis \vec{l} of the α Per cluster in the rotated system ($O'_r-X'_rY'_rZ'_r$), i.e., $(\alpha', \beta', \gamma') = (138^\circ, 133^\circ, 230^\circ)$. Then, the PAs of $(\alpha, \beta, \gamma) = (68^\circ, 51^\circ, 26^\circ)$ for \vec{l} in the $O_c-X_cY_cZ_c$ system can be obtained by using Equation (1). Thus, \vec{l} is tilted at an angle of $48^\circ \pm 14^\circ$ with respect to the Galactic plane. With the PAs, we derive the vectors of the X_r , Y_r , and Z_r axes of the $O_r-X_rY_rZ_r$ system in the $O_c-X_cY_cZ_c$ system. After transforming the 3D coordinates and velocity components of the cluster members from the $O_c-X_cY_cZ_c$ system to those in the $O_r-X_rY_rZ_r$ system, we also calculate the 3D coordinates (r, φ, z) and velocity components (v_r, v_φ, v_z) of the cluster members in the cylindrical coordinate system. As for the Pleiades, using the rotation velocities (v_φ) and uncertainties of the member stars, we estimate the mean rotation velocity of the α Per cluster within its tidal radius to be $0.43 \pm 0.08 \text{ km s}^{-1}$, which is in consistent with the results shown in Figures 7.

4.3.2. Rotational properties of the stars in α Per

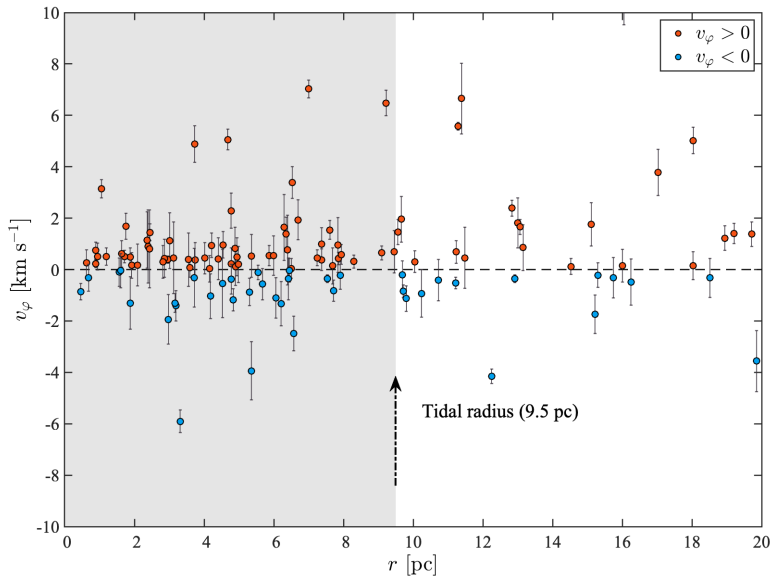


Figure 8. Rotational velocity as a function of distance to the cluster center, for the member stars within two times of the tidal radius of the α Per.

The rotational velocities of the member stars as a function of their distances to the cluster center are presented in Figure 8. Similar to the Presepe (Paper I) and the Pleiades (this paper), not all of the member stars of the α Per cluster rotate in the same direction. The ratio of the number of members with positive v_φ values to those with negative values is ~ 2.3 , which is higher than that of the Pleiades. Due to the tidal force of the Milky Way, the rotation of the member stars located beyond the cluster tidal radius (9.5 pc) seems to be disordered, as shown in Figure 8. Moreover, in a few stars, the peculiar rotational velocities deviate from those of most cluster members within the tidal radius of the α Per.

Understanding the rotational patterns of the member stars within the tidal radius of the α Per cluster is an intriguing issue. To this end, we compare our observations with the theoretical predictions of Newton's theorems, following the

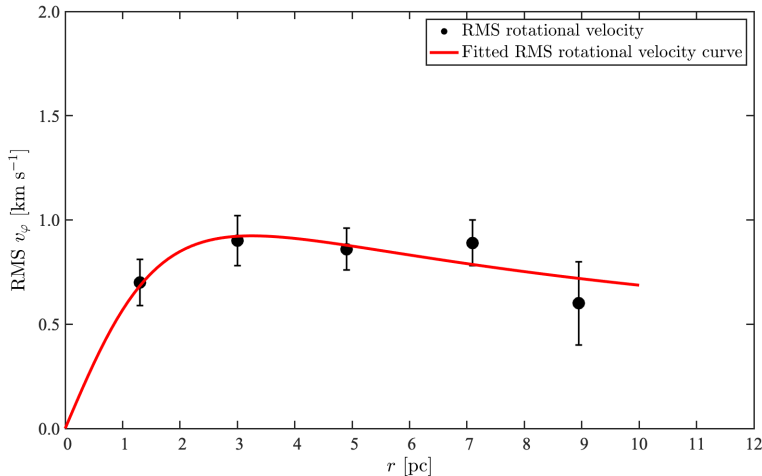


Figure 9. RMS rotational velocity as a function of distance to the center of the α Per cluster. The black dots denote the observed RMS rotational velocities of the member stars, with uncertainties indicated by error bars. The red line is the best-fitting curve for the observed RMS rotational velocities according to the Newton’s theorems.

Table 6. RMS rotational velocities of the member stars within the tidal radius of the α Per cluster.

R_i [pc]	R_o [pc]	R_m [pc]	N	RMS v_φ [km s $^{-1}$]	$\epsilon_{\text{RMS } v_\varphi}$ [km s $^{-1}$]
(1)	(2)	(3)	(4)	(5)	(6)
0.0	2.0	1.3	15	0.70	0.11
2.0	4.0	3.0	17	0.90	0.12
4.0	6.0	4.9	21	0.89	0.10
6.0	8.0	7.1	21	0.86	0.11
8.0	9.5	8.9	3	0.58	0.24

NOTE—The same format as Table 4, but for the α Per cluster.

same analysis procedure as for the Pleiades. Within the tidal radius of the α Per, the skewness of the Galactic longitudes, Galactic latitudes, and parallaxes of member stars are 0.2, 0.2, and -0.4 , respectively, indicating that the assumption of the spherically symmetric distribution in the cluster is reasonable. Next, we try to use Equation (2) to describe the RMS rotational velocity derived from the member stars of the α Per cluster.

Within the tidal radius of the α Per cluster, there are 85 member stars in the sample. The median absolute value of their rotation velocities v_φ is ~ 0.6 km s $^{-1}$, with a standard deviation of ~ 1.4 km s $^{-1}$. For these member stars, we study their rotational characteristics by dividing them into several bins according to their distances from the cluster center. Eight stars with peculiar rotational velocities deviating from the overall velocity are eliminated. Similar to the Pleiades, using the remaining 77 member stars, we calculate the RMS rotation velocity and uncertainty in each distance bin. The results are given in Table 6 and Figure 9. The RMS rotational velocities of the member stars can be well fit by the velocity profile of circular motion expected by Newton’s theorems, suggesting that the rotation of the member stars within the tidal radius of the α Per can be elucidated by Newton’s theorems. The core radius and the mass within the tidal radius of the α Per cluster is 2.3 ± 0.5 pc and $1186 \pm 312 M_\odot$, respectively, derived by fitting the RMS velocities listed in Table 6 with Equation (2), with the same technique for the Pleiades. We find that the best-fitting core radius matches the result of 2.3 ± 0.3 pc reported by Lodieu et al. (2019a), but is significantly smaller than the early estimate (~ 4 pc, see Artyukhina 1972; Kharchenko et al. 2005).

The age of the α Per cluster has been estimated to be approximately 50–70 Myr (see Section 1). As presented in Figure 10, the mean radial components \bar{v}_r of the member stars within $0.5 r_{\text{td}}$, $1 r_{\text{td}}$, and $3 r_{\text{td}}$ are 0.0 ± 0.09 , 0.1 ± 0.07 , and 0.1 ± 0.06 km s $^{-1}$, respectively, using the same approach as for the Pleiades. In this context, we posit that the α Per cluster shows no obvious signs of expansion or contraction, suggesting that the rotation of the member stars within the tidal radius exhibits closed-loop motions. Additionally, as for the Pleiades, the above estimated mass

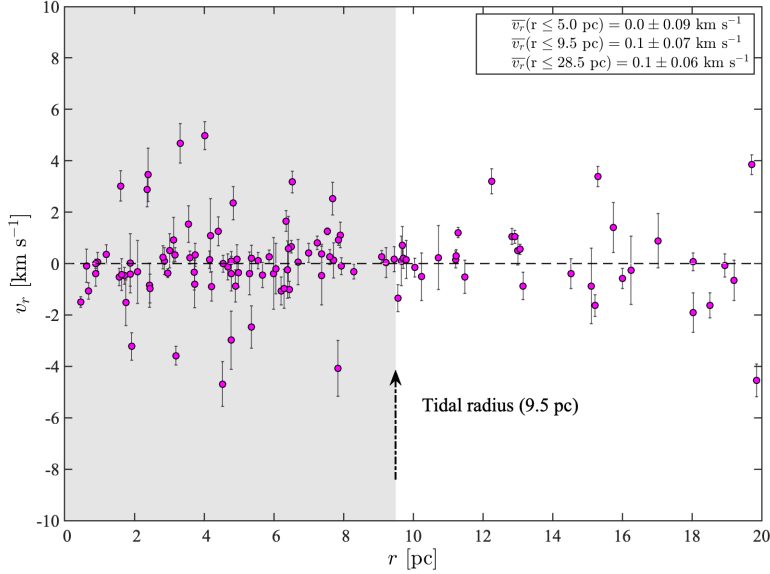


Figure 10. Same as Figure 5, but for the α Per cluster.

of the α Per is expected to be a lower limit, since the non-negligible radial component acceleration and dispersion (Figure 10) of the cluster members imply that the cluster ought to have additional mass.

4.4. The Hyades cluster

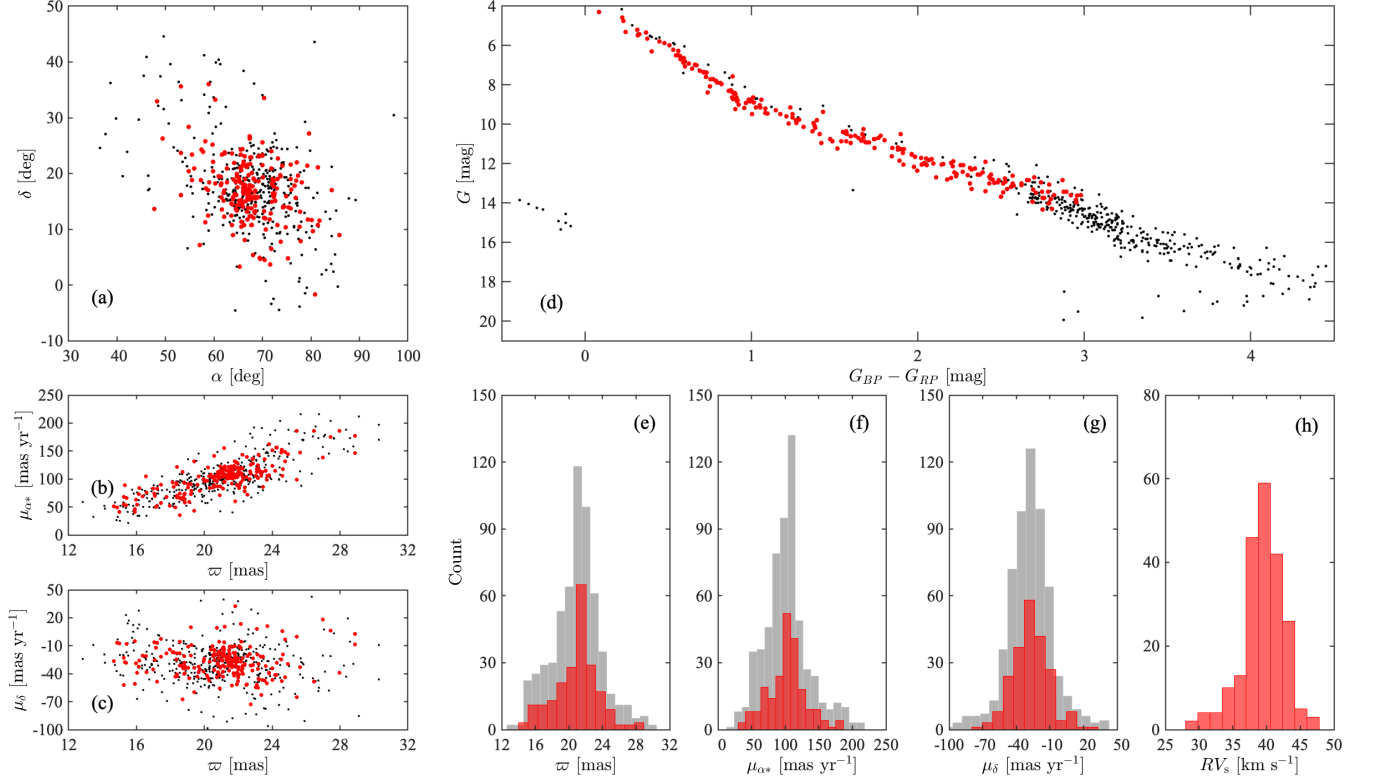
In Figure 11, we display the multidimensional distributions and color-magnitude diagram for the Hyades cluster. In this section, we picture the rotation in the Hyades cluster, and investigate the rotational characteristics of the member stars.

4.4.1. Rotation in Hyades

For the subsample of 214 member stars with radial velocities (see Table 1), the median uncertainties of parallax, proper motion μ_{α^*} and μ_{δ} are 0.02 mas, 0.03 mas yr⁻¹, and 0.02 mas yr⁻¹, respectively. The median uncertainty of the radial velocity is 0.3 km s⁻¹. From these member stars, we estimate the means and standard deviations of the basic parameters of the Hyades cluster to be: (R.A., Decl.)=(67.41° ± 6.50°, 17.18° ± 5.69°), $\varpi = 20.99 \pm 2.61$ mas, $(\mu_{\alpha^*}, \mu_{\delta}) = (102.68 \pm 27.97, -27.25 \pm 16.30)$ mas yr⁻¹, and RV = 39.39 ± 3.10 km s⁻¹, in concordance with previous results (Perryman et al. 1998; van Leeuwen 2009; Majaess et al. 2011; Lodieu et al. 2019b). With these parameters, we calculate the center, 3D motions, and corresponding uncertainties of the Hyades cluster in the Galactic $O_g-X_gY_gZ_g$ system. For each member of the Hyades, we first calculate its 3D coordinates, 3D motions, and corresponding uncertainties in the Galactic coordinate system, and we then transform them into the $O_c-X_cY_cZ_c$ system.

As in the case of the α Per, we can determine the rotation signals in the Hyades by using the residual velocity method in the $O_c-X_cY_cZ_c$ system, but we can not pin down the PAs (α, β, γ) of the rotation axis \vec{l} . Using a set of PAs $(\alpha_0, \beta_0, \gamma_0) = (10^\circ, 10^\circ, 45^\circ)$, the 3D coordinates and velocity components of the cluster members are transformed from the $O_c-X_cY_cZ_c$ system to the rotated $O_r-X_rY_rZ_r$ system. We then determine the PAs of the rotation axis \vec{l} (α', β', γ') in the rotated system by using the same method as for the aforementioned clusters. In Figure 12, we display the mean residual velocities as functions of PAs, using the member stars within 3 r_{td} (a-c), 1 r_{td} (d-f), and 0.5 r_{td} (g-i) of the Hyades cluster. According to Lodieu et al. (2019b), the Hyades cluster has a tidal radius of 9.0 pc. The sinusoidal behavior of the mean residual velocities as a function of PAs is an excellent indication of the 3D rotation of the Hyades cluster, although the result in Figure 12(a) is not very significant.

Table 7 and Figure 12 summarize the fitted PAs (α', β', γ') of the rotation axis \vec{l} of the Hyades in the rotated system. Like the Pleiades, the PAs obtained by using the member stars within the tidal radius of the Hyades are concordant with those obtained by using the members within half of the tidal radius, and they all satisfy the relation of $\tan \alpha \cdot \tan \gamma = \tan \beta$ considering the uncertainties. In contrast, the PAs derived by using the member stars within


Figure 11. Same as Figure 1, but for the Hyades cluster.

three times of the tidal radius are different from the above results, although they also satisfy $\tan \alpha \cdot \tan \gamma = \tan \beta$ considering the uncertainties. This phenomenon has also been shown for the Praesepe and Pleiades clusters.

For the Hyades cluster, the PAs obtained by the members within the tidal radius are exploited to determine the rotation axis \vec{l} . Considering the relation $\tan \alpha' \cdot \tan \gamma' = \tan \beta'$, we adopt the PAs of $(\alpha', \beta', \gamma') = (87^\circ, 90^\circ, 96^\circ)$ to obtain the vectors of the rotation axis \vec{l} in the $O_c-X_cY_cZ_c$ system, and we then use Equation (1) to determine the PAs of the rotation axis \vec{l} in the $O_r-X_rY_rZ_r$ system to be $(\alpha, \beta, \gamma) = (10^\circ, 11^\circ, 48^\circ)$. We find that the rotation axis of the Hyades cluster is nearly parallel to the Galactic plane, with an estimated angle of $7^\circ \pm 7^\circ$. The vectors of the X_r , Y_r , and Z_r axes of the $O_r-X_rY_rZ_r$ system in the $O_c-X_cY_cZ_c$ system can be given by the PAs (α, β, γ) . Subsequently, we transform the 3D coordinates and velocity components of the cluster members from the $O_c-X_cY_cZ_c$ system to the $O_r-X_rY_rZ_r$ system, and we finally obtain the 3D coordinates (r, φ, z) and velocity components (v_r, v_φ, v_z) of the cluster members in the cylindrical coordinate system. Using the same technique as the previous two clusters, averaging the rotation velocities (v_φ) of the member stars yields a rotation velocity of $0.09 \pm 0.03 \text{ km s}^{-1}$ for the Hyades cluster, in agreement with the results shown in Figures 12.

Table 7. Best-fit PAs of the Hyades cluster.

	α'	β'	γ'
$3.0 r_{\text{td}}$	$176^\circ \pm 26^\circ$	$53^\circ \pm 23^\circ$	$312^\circ \pm 28^\circ$
$1.0 r_{\text{td}}$	$87^\circ \pm 14^\circ$	$96^\circ \pm 20^\circ$	$96^\circ \pm 17^\circ$
$0.5 r_{\text{td}}$	$85^\circ \pm 6^\circ$	$96^\circ \pm 36^\circ$	$82^\circ \pm 27^\circ$

NOTE— r_{td} : tidal radius of the Hyades cluster.

4.4.2. Rotational properties of stars in Hyades

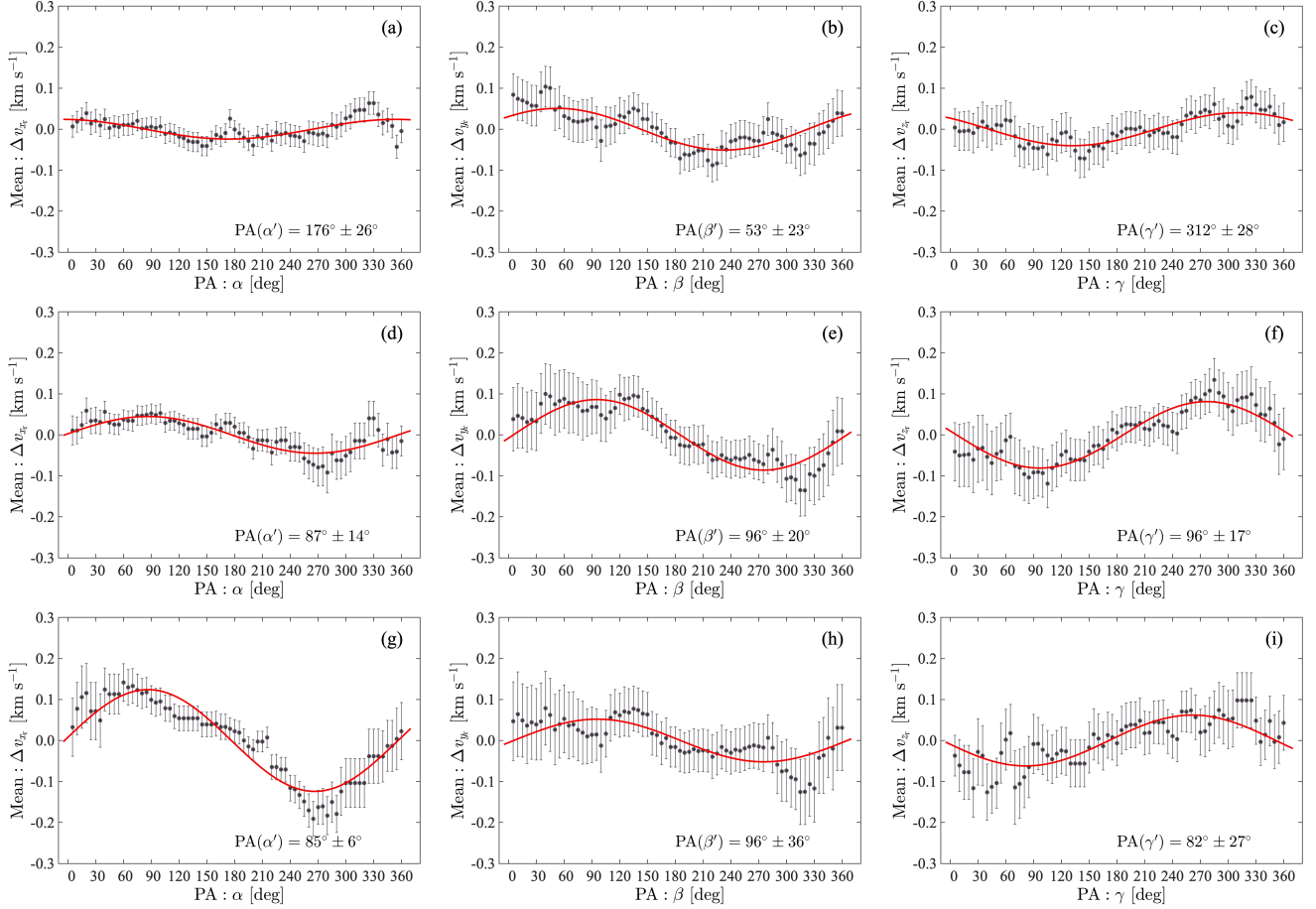


Figure 12. Same as Figure 2, but for the Hyades cluster.

Figure 13 shows the variation in the rotational velocities of the member stars of the Hyades cluster vary with their distance to the cluster center. Similar to the properties of the former two clusters, not all member stars rotate in the same direction. The number of the member stars with positive rotational velocities is 1.4 times of those with negative rotational velocities. Compared with the Pleiades and the α Per cluster, there are fewer member stars have peculiar rotational velocities that deviate from that of most cluster members within the tidal radius of the Hyades. In addition, the rotation of the member stars located near or beyond the tidal radius does not appear to be disorganized, as seen from Figure 13.

In the same way as for the Pleiades and α Per, the skewness of the astrometric parameters of the member stars within the tidal radius of the Hyades cluster are calculated to assess the symmetry of the cluster density distribution. The skewness of the Galactic longitude, Galactic latitude, and parallax are 0.1, 0.1, and 0.0, respectively, indicating that it makes sense for us to assume a spherically symmetric distribution in the Hyades.

In the sample, 163 member stars lie within the tidal radius of the Hyades cluster. The median absolute value of their rotational velocities v_φ is $\sim 0.5 \text{ km s}^{-1}$ with a standard deviation of $\sim 0.5 \text{ km s}^{-1}$. Similar to the analysis for the Pleiades and the α Per cluster, we first eliminate 7 stars with peculiar rotational velocities after inspecting the distribution of rotational velocities of the member stars. Then, using the remaining 156 member stars, we calculate the RMS rotation velocity and uncertainty for the members within each distance bin. The results are given in Table 8 and Figure 14. Using Equation (2), the RMS rotational velocities as a function of the distances to the cluster center are well fit by a theoretical circular motion velocity curve. Therefore, it may be feasible to describe the rotation of the member stars within the tidal radius of the Hyades using Newton's theorems. Furthermore, with the same method as for the above two clusters, after using Equation (2) to fit the RMS velocities listed in Table 8, we infer that the core radius and mass within the tidal radius of the Hyades cluster are $2.1 \pm 0.3 \text{ pc}$ and $569 \pm 108 M_\odot$, respectively.

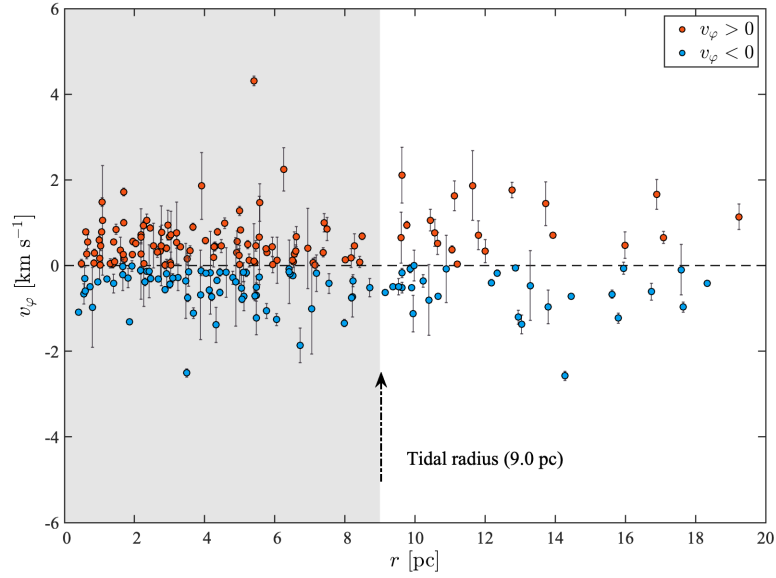


Figure 13. Rotational velocity as a function of distance to the cluster center for the member stars within twice of the tidal radius of the Hyades.

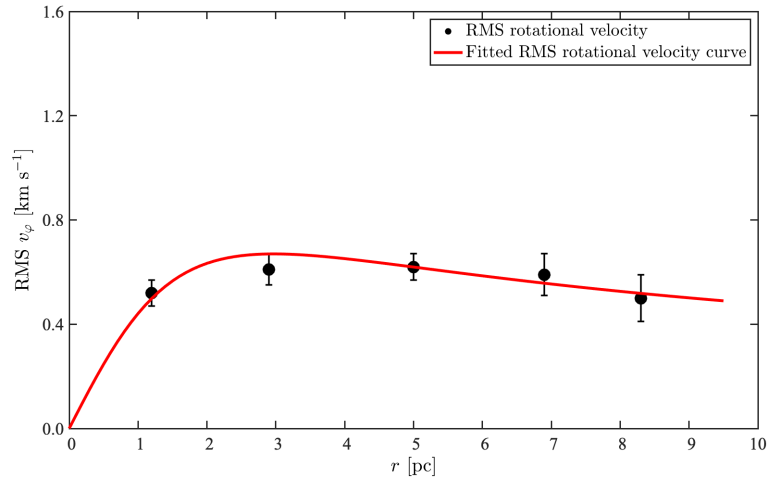


Figure 14. Same as Figure 9, but for the Hyades cluster.

Table 8. RMS rotational velocities of the members stars within the tidal radius of the Hyades cluster.

R_i [pc]	R_o [pc]	R_m [pc]	N	RMS v_ϕ [km s $^{-1}$]	$\epsilon_{\text{RMS } v_\phi}$ [km s $^{-1}$]
(1)	(2)	(3)	(4)	(5)	(6)
0.0	2.0	1.2	36	0.52	0.05
2.0	4.0	2.9	44	0.61	0.06
4.0	6.0	5.0	46	0.62	0.05
6.0	8.0	6.9	21	0.59	0.08
8.0	9.5	8.3	9	0.50	0.09

NOTE—The same format as Table 4, but for the Hyades cluster.

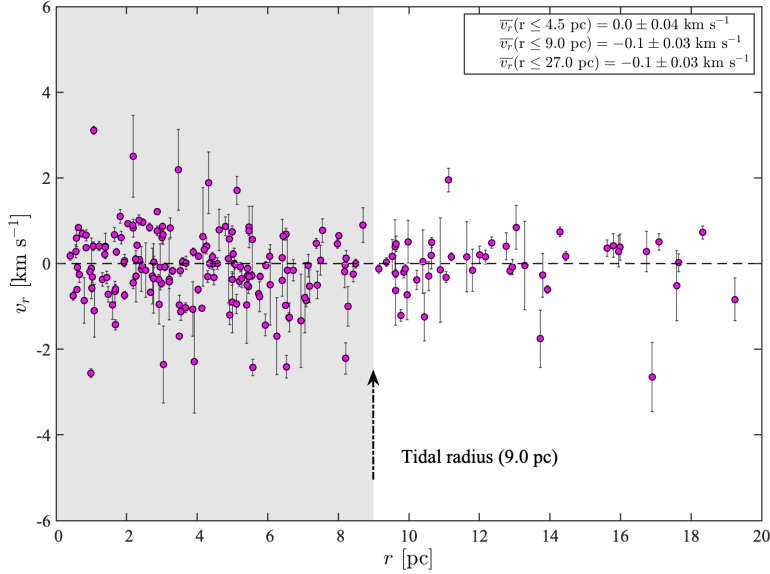


Figure 15. Same as Figure 5, but for the Hyades cluster.

We also examine whether the Hyades cluster, an OC with an age of about 650 Myr (see Section 1), is expanding or contracting by statistically analyzing the radial components v_r of the member stars. As indicated in Figure 15, the mean radial components \bar{v}_r of the member stars within $0.5 r_{\text{td}}$, $1 r_{\text{td}}$, and $3 r_{\text{td}}$ are 0.0 ± 0.04 , -0.1 ± 0.03 , and -0.1 ± 0.03 km s^{-1} , respectively. Similar to the Pleiades and the α Per cluster, the mean radial components are also close to zero. These results suggest that there is no significant expansion or contraction in the Hyades, and this implies that the rotation of the cluster members within the tidal radius may exhibit closed-loop motions. Figure 15 also shows that the member stars of the Hyades cluster show non-negligible acceleration and dispersion in their radial components, indicating that there should be additional mass in the system to account for the force supporting the radial component acceleration. Therefore, the estimated mass in this work is a lower limit for the Hyades.

5. DISCUSSION

Table 9. Parameters of the Praesepe, Pleiades, α Per, and the Hyades.

	Rotational velocity [km s^{-1}]	\vec{l} vs. GP [degree]	<i>Dist.</i> [pc]	Mass M_{\odot}	Age [Myr]	$r_{\text{td}} (r_{\text{co}})$ [pc]	$ Z $ [pc]
Praesepe	0.12 ± 0.05	34 ± 15	$178 \pm 0.8^{[1]}$	$\sim 510^{[3]}$	590–700 ^[1,7]	10.7(2.6) ^[1]	$101 \pm 2.2^{[1]}$
Pleiades	0.24 ± 0.04	62 ± 13	$135 \pm 0.4^{[1]}$	$\sim 820^{[4]}$	110–160 ^[1,7]	11.6(2.0) ^[1]	$55 \pm 0.2^{[1]}$
α Per	0.43 ± 0.08	48 ± 14	$187 \pm 3.9^{[1]}$	$\sim 920^{[5]}$	50–70 ^[8,9]	9.5(2.3) ^[1]	$20 \pm 0.5^{[1]}$
Hyades	0.09 ± 0.03	7 ± 7	$47 \pm 0.2^{[2]}$	$\sim 280^{[6]}$	650–780 ^[2,10]	9.0(3.1) ^[2]	$17 \pm 0.1^{[2]}$

NOTE—¹ Lodieu et al. (2019a), ² Lodieu et al. (2019b), ³ Loktin & Popov (2020), ⁴ Almeida et al. (2023), ⁵ Nikiforova et al. (2020), ⁶ Röser et al. (2011), ⁷ Gossage et al. (2018), ⁸ Prosser et al. (1996), ⁹ Makarov (2006), ¹⁰ Brandner et al. (2023). \vec{l} : rotation axis. GP: Galactic plane. \vec{l} vs. GP: the included angle between the rotation axis and the Galactic plane. *Dist.*: distance to the Sun. r_{td} : tidal radius. r_{co} : core radius. $|Z|$: z -scale heights from the Galactic plane.

Based on *Gaia* DR3, we investigate the 3D internal rotation of four nearby member-rich OCs and estimate their rotation axes and mean rotational velocities. Interestingly, Newton’s theorem can well interpret the rotation of member stars within the tidal radii of these OCs. In addition, no indication of expansion or contraction has been detected in the four OCs, in agreement with the result of Della Croce et al. (2023), who reported that the clusters older than 30 Myr do not experience expansion and are mostly compatible with equilibrium configurations. Although the sample size is

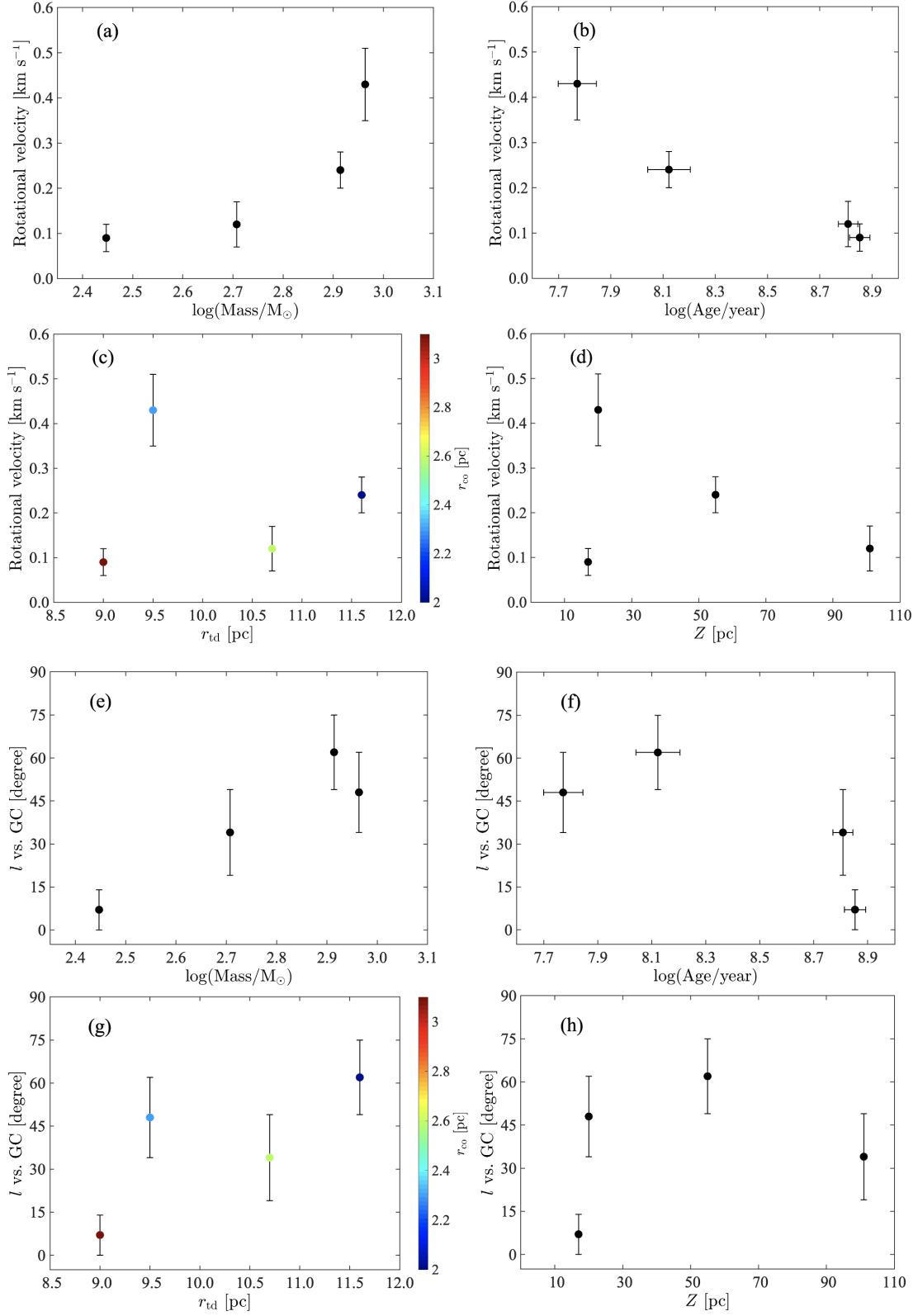


Figure 16. Panels (a), (b), (c), and (d): rotational velocities of the Praesepe, Pleiades, α Per, and the Hyades clusters as functions of their masses, ages, radii (r_{td} , r_{co}), and z -scale heights (Z) from the Galactic plane. Panels (e), (f), (g), and (h): the same as Panels (a-d), but for the angles of the cluster rotation axes (\vec{l}) with respect to the Galactic plane.

small, Praesepe, the Pleiades, α Per, and the Hyades are currently the only four OCs with a determined 3D rotation, which makes it feasible to explore the possible relations between the rotation of OCs and other cluster parameters. In Table 9, we compile the distances, masses, ages, radii, and z -scale heights of these four OCs from the literature. The cluster rotational velocities and rotation axes given by this work are also listed. Clearly, the rotational parameters of the OCs have no obvious relation with the cluster distances from the Sun. The results for the other cluster parameters are given in Figure 16.

Figure 16(a-d) present the variation in the rotational velocities with other cluster parameters. It is shown in Figure 16(a) that OCs with higher masses tend to have greater rotational velocities, implying that the rotational velocity of OCs may be positively correlated with their masses. In fact, the Galactic globular clusters, as the stellar populations that are much more massive than OCs, are observed to have internal rotation velocities of several km s^{-1} (e.g., Lanzoni et al. 2018; Leanza et al. 2022), which is one order of magnitude higher than these four OCs. In Figure 16(b), it is interesting to note that young OCs have higher rotation velocities than old OCs, which suggests that the rotational velocity of OCs may gradually decrease as they age. If this is the case, the present-day rotation of OCs is likely to originate from their predecessor clusters, whose rotation is found to be common in hydrodynamical simulations (e.g., Mapelli 2017). With the available data, we do not find any clear relation between the rotational velocities and the tidal radii or the z -scale heights of OCs.

Figure 16(e-h) present the included angles between the cluster rotation axes and the Galactic plane as a function of cluster parameters. In Figure 16(e), we find that the included angles of the massive OCs appear to be larger than those of the low-mass OCs. In comparison with old OCs, the younger OCs seem to have larger included angles, as shown in Figure 16(f). The above two relations are not significant when the errors of the included angles are taken into account. Based on these four clusters, no clear correlations can be identified between the directions of the rotation axes and the cluster radii or the cluster z -scale heights, as shown in Figure 16(g) and (h).

So far, we have only studied the 3D rotation of four star-rich OCs within 200 pc from the Sun. The sample size is very limited. The above results need to be further confirmed by the rotational characteristics of more OCs. An accurate detection of 3D rotation in more distant star-rich OCs (such as those clusters located within 500 pc) requires high-precision astrometry and improved methods. More efforts will be undertaken to reveal the internal 3D rotation of more OCs, which will help us to improve our understanding of the formation and evolution of OCs in the Milky Way.

6. SUMMARY

We report significant detections of rotation in the Pleiades, α Per, and Hyades clusters based on the high-quality data of *Gaia* DR3. In order to unveil the internal kinematics of star clusters, we have slightly amended the method developed in our previous work (Paper I). The analyses on the motions of the member stars not only revealed 3D rotation of the Pleiades, α Per, and the Hyades, but also determined their rotation axes in the Milky Way, with angles of $62^\circ \pm 13^\circ$, $48^\circ \pm 14^\circ$, and $7^\circ \pm 7^\circ$ relative to the Galactic plane, respectively. We also unveil the rotational properties of the member stars in the three OCs and suggest that the theorems of Newtonian mechanics can well characterize the rotational velocities of the member stars within each cluster tidal radius. In addition, the statistics of current observations suggest that the three clusters do not expand or contract.

Combining the Praesepe cluster analyzed in Paper I with the three OCs investigated in this work, we find a possible relation between the rotational velocity and the age and mass of the cluster. Massive OCs tend to have significant internal rotation, and the rotation velocity gradually decreases from young to old OCs. However, these results need to be further confirmed when the rotational features of more clusters are revealed. To date, the internal kinematics of almost all known OCs remain elusive, leaving a major gap in the study of star clusters in the Milky Way. The method reported in this work takes a step in the direction of unveiling the detailed kinematic properties of OCs. The 3D rotations of OCs has been measured based on the high-precision parallaxes, proper motions, radial velocities from the *Gaia* DR3 dataset. With the improvement of astrometric accuracy and precision in the upcoming *Gaia* Data Releases, it is expected that there will be a wealth of yet-to-be-revealed interesting kinematic properties of OCs, deserving our attention and exploration.

ACKNOWLEDGMENTS

We thank the anonymous referee for the instructive comments and suggestions that greatly helped us to improve the paper. This work was funded by the NSFC grant 11933011, 11988101, National SKA Program of China (grant No. 2022SKA0120103), and the Key Laboratory for Radio Astronomy. L.G.H. acknowledges the support from the Youth Innovation Promotion Association CAS. Y.J.L. acknowledges support from the NSFC grant 12203104 and the Natural Science Foundation of Jiangsu Province (grant No. BK20210999). We used data from the European Space Agency mission *Gaia* (<http://www.cosmos.esa.int/gaia>), processed by the *Gaia* Data Processing and Analysis Consortium (DPAC; see <http://www.cosmos.esa.int/web/gaia/dpac/consortium>). Funding for DPAC has been provided by national institutions, in particular, the institutions participating in the *Gaia* Multilateral Agreement.

APPENDIX

Figure A1 presents the definitions of the $O_c-X_cY_cZ_c$ and the $O_r-X_rY_rZ_r$ systems.

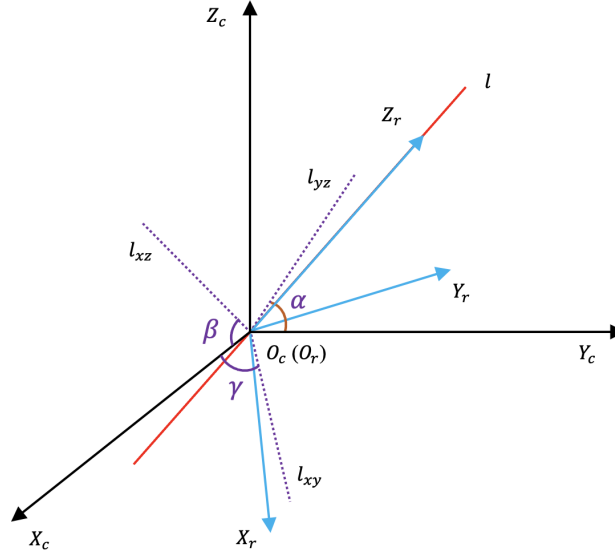


Figure A1. Definitions of the $O_c-X_cY_cZ_c$ (black) system and the $O_r-X_rY_rZ_r$ (blue) system (from Paper I). The cluster rotation axis \vec{l} (red) is in accordance with the Z_r axis. The projections of \vec{l} in the Y_c-Z_c , X_c-Z_c , and X_c-Y_c planes are l_{yz} , l_{xz} , and l_{xy} (purple), respectively. The projection of the X_r -axis in the X_c-Y_c plane is consistent with l_{xy} . α , β and γ indicate the included angles between l_{yz} and Y_c , l_{xz} and X_c , and l_{xy} and X_c , respectively.

REFERENCES

- Almeida, A., Monteiro, H., & Dias, W. S. 2023, MNRAS, 525, 2315, doi: [10.1093/mnras/stad2291](https://doi.org/10.1093/mnras/stad2291)
- An, D., Terndrup, D. M., Pinsonneault, M. H., et al. 2007, ApJ, 655, 233, doi: [10.1086/509653](https://doi.org/10.1086/509653)
- Artyukhina, N. M. 1972, Soviet Ast., 16, 317
- Basri, G., Marcy, G. W., & Graham, J. R. 1996, ApJ, 458, 600, doi: [10.1086/176842](https://doi.org/10.1086/176842)
- Bastian, N., & Goodwin, S. P. 2006, MNRAS, 369, L9, doi: [10.1111/j.1745-3933.2006.00162.x](https://doi.org/10.1111/j.1745-3933.2006.00162.x)
- Brandner, W., Calissendorff, P., & Kopytova, T. 2023, AJ, 165, 108, doi: [10.3847/1538-3881/acb208](https://doi.org/10.3847/1538-3881/acb208)
- Bressert, E., Bastian, N., Gutermuth, R., et al. 2010, MNRAS, 409, L54, doi: [10.1111/j.1745-3933.2010.00946.x](https://doi.org/10.1111/j.1745-3933.2010.00946.x)
- Castro-Ginard, A., Jordi, C., Luri, X., et al. 2022, A&A, 661, A118, doi: [10.1051/0004-6361/202142568](https://doi.org/10.1051/0004-6361/202142568)
- Collinder, P. 1931, Annals of the Observatory of Lund, 2, B1

- Converse, J. M., & Stahler, S. W. 2008, *ApJ*, 678, 431, doi: [10.1086/529431](https://doi.org/10.1086/529431)
- . 2010, *MNRAS*, 405, 666, doi: [10.1111/j.1365-2966.2010.16505.x](https://doi.org/10.1111/j.1365-2966.2010.16505.x)
- Dahm, S. E. 2015, *ApJ*, 813, 108, doi: [10.1088/0004-637X/813/2/108](https://doi.org/10.1088/0004-637X/813/2/108)
- De Gennaro, S., von Hippel, T., Jefferys, W. H., et al. 2009, *ApJ*, 696, 12, doi: [10.1088/0004-637X/696/1/12](https://doi.org/10.1088/0004-637X/696/1/12)
- Della Croce, A., Dalessandro, E., Livernois, A. R., & Vesperini, E. 2023, arXiv e-prints, arXiv:2312.02263, doi: [10.48550/arXiv.2312.02263](https://doi.org/10.48550/arXiv.2312.02263)
- Elmegreen, B. G., & Clemens, C. 1985, *ApJ*, 294, 523, doi: [10.1086/163320](https://doi.org/10.1086/163320)
- Farias, J. P., Fellhauer, M., Smith, R., Domínguez, R., & Dabringhausen, J. 2018, *MNRAS*, 476, 5341, doi: [10.1093/mnras/sty597](https://doi.org/10.1093/mnras/sty597)
- Gaia Collaboration, Prusti, T., de Bruijne, J. H. J., et al. 2016, *A&A*, 595, A1, doi: [10.1051/0004-6361/201629272](https://doi.org/10.1051/0004-6361/201629272)
- Gaia Collaboration, Babusiaux, C., van Leeuwen, F., et al. 2018, *A&A*, 616, A10, doi: [10.1051/0004-6361/201832843](https://doi.org/10.1051/0004-6361/201832843)
- Gaia Collaboration, Brown, A. G. A., Vallenari, A., et al. 2021, *A&A*, 649, A1, doi: [10.1051/0004-6361/202039657](https://doi.org/10.1051/0004-6361/202039657)
- Gaia Collaboration, Vallenari, A., Brown, A. G. A., et al. 2023, *A&A*, 674, A1, doi: [10.1051/0004-6361/202243940](https://doi.org/10.1051/0004-6361/202243940)
- Gao, X.-h. 2019, *PASP*, 131, 044101, doi: [10.1088/1538-3873/ab010e](https://doi.org/10.1088/1538-3873/ab010e)
- Gatewood, G., de Jonge, J. K., & Han, I. 2000, *ApJ*, 533, 938, doi: [10.1086/308679](https://doi.org/10.1086/308679)
- Gossage, S., Conroy, C., Dotter, A., et al. 2018, *ApJ*, 863, 67, doi: [10.3847/1538-4357/aad0a0](https://doi.org/10.3847/1538-4357/aad0a0)
- Guilherme-Garcia, P., Krone-Martins, A., & Moitinho, A. 2023, *A&A*, 673, A128, doi: [10.1051/0004-6361/202142826](https://doi.org/10.1051/0004-6361/202142826)
- Hao, C. J., Xu, Y., Bian, S. B., et al. 2022a, *ApJ*, 938, 100, doi: [10.3847/1538-4357/ac92fc](https://doi.org/10.3847/1538-4357/ac92fc)
- Hao, C. J., Xu, Y., Hou, L. G., Lin, Z. H., & Li, Y. J. 2023, *Research in Astronomy and Astrophysics*, 23, 075023, doi: [10.1088/1674-4527/acd58d](https://doi.org/10.1088/1674-4527/acd58d)
- Hao, C. J., Xu, Y., Wu, Z. Y., et al. 2022b, *A&A*, 660, A4, doi: [10.1051/0004-6361/202243091](https://doi.org/10.1051/0004-6361/202243091)
- Healy, B. F., McCullough, P. R., & Schlaufman, K. C. 2021, *ApJ*, 923, 23, doi: [10.3847/1538-4357/ac281d](https://doi.org/10.3847/1538-4357/ac281d)
- Hunt, E. L., & Reffert, S. 2023, *A&A*, 673, A114, doi: [10.1051/0004-6361/202346285](https://doi.org/10.1051/0004-6361/202346285)
- Gaia Collaboration, Brown, A. G. A., Vallenari, A., et al. 2018, *A&A*, 616, A1, doi: [10.1051/0004-6361/201833051](https://doi.org/10.1051/0004-6361/201833051)
- Jones, B. F. 1981, *AJ*, 86, 290, doi: [10.1086/112887](https://doi.org/10.1086/112887)
- Kamann, S., Bastian, N. J., Gieles, M., Balbinot, E., & Hénault-Brunet, V. 2019, *MNRAS*, 483, 2197, doi: [10.1093/mnras/sty3144](https://doi.org/10.1093/mnras/sty3144)
- Kharchenko, N. V., Piskunov, A. E., Röser, S., Schilbach, E., & Scholz, R. D. 2005, *A&A*, 438, 1163, doi: [10.1051/0004-6361:20042523](https://doi.org/10.1051/0004-6361:20042523)
- Lada, C. J., & Lada, E. A. 2003, *ARA&A*, 41, 57, doi: [10.1146/annurev.astro.41.011802.094844](https://doi.org/10.1146/annurev.astro.41.011802.094844)
- Lanzoni, B., Ferraro, F. R., Mucciarelli, A., et al. 2018, *ApJ*, 861, 16, doi: [10.3847/1538-4357/aac26a](https://doi.org/10.3847/1538-4357/aac26a)
- Leanza, S., Pallanca, C., Ferraro, F. R., et al. 2022, *ApJ*, 929, 186, doi: [10.3847/1538-4357/ac5d4e](https://doi.org/10.3847/1538-4357/ac5d4e)
- Liu, T., Janes, K. A., & Bania, T. M. 1991, *ApJ*, 377, 141, doi: [10.1086/170342](https://doi.org/10.1086/170342)
- Lodieu, N., Pérez-Garrido, A., Smart, R. L., & Silvotti, R. 2019a, *A&A*, 628, A66, doi: [10.1051/0004-6361/201935533](https://doi.org/10.1051/0004-6361/201935533)
- Lodieu, N., Rebolo, R., & Pérez-Garrido, A. 2018, *A&A*, 615, L12, doi: [10.1051/0004-6361/201832748](https://doi.org/10.1051/0004-6361/201832748)
- Lodieu, N., Smart, R. L., Pérez-Garrido, A., & Silvotti, R. 2019b, *A&A*, 623, A35, doi: [10.1051/0004-6361/201834045](https://doi.org/10.1051/0004-6361/201834045)
- Loktin, A. V., & Popov, A. A. 2020, *AN*, 341, 638, doi: [10.1002/asna.202013687](https://doi.org/10.1002/asna.202013687)
- Lynga, G. 1981, *Astronomical Data Center Bulletin*, 1, 90
- Maeder, A., & Mermilliod, J. C. 1981, *A&A*, 93, 136
- Majaess, D. J., Turner, D. G., Lane, D. J., & Krajci, T. 2011, *JAASO*, 39, 219, doi: [10.48550/arXiv.1102.1705](https://doi.org/10.48550/arXiv.1102.1705)
- Makarov, V. V. 2006, *AJ*, 131, 2967, doi: [10.1086/503900](https://doi.org/10.1086/503900)
- Mapelli, M. 2017, *MNRAS*, 467, 3255, doi: [10.1093/mnras/stx304](https://doi.org/10.1093/mnras/stx304)
- McArthur, B. E., Benedict, G. F., Harrison, T. E., & van Altena, W. 2011, *AJ*, 141, 172, doi: [10.1088/0004-6256/141/5/172](https://doi.org/10.1088/0004-6256/141/5/172)
- Megeath, S. T., Gutermuth, R., Muzerolle, J., et al. 2016, *AJ*, 151, 5, doi: [10.3847/0004-6256/151/1/5](https://doi.org/10.3847/0004-6256/151/1/5)
- Melis, C., Reid, M. J., Mioduszewski, A. J., Stauffer, J. R., & Bower, G. C. 2014, *Science*, 345, 1029, doi: [10.1126/science.1256101](https://doi.org/10.1126/science.1256101)
- Melotte, P. J. 1915, *MmRAS*, 60, 175
- Mermilliod, J. C. 1981, *A&A*, 97, 235
- Mermilliod, J. C., Bratschi, P., & Mayor, M. 1997, *A&A*, 320, 74
- Mermilliod, J. C., Mayor, M., & Udry, S. 2008, *A&A*, 485, 303, doi: [10.1051/0004-6361:200809664](https://doi.org/10.1051/0004-6361:200809664)
- Messier, C. 1781, *Catalogue des Nébuleuses et des Amas d'Étoiles (Catalog of Nebulae and Star Clusters)*, Connaissance des Temps ou des Mouvements Célestes, for 1784, p. 227-267
- Nikiforova, V. V., Kulesh, M. V., Seleznev, A. F., & Carraro, G. 2020, *AJ*, 160, 142, doi: [10.3847/1538-3881/aba753](https://doi.org/10.3847/1538-3881/aba753)

- Perryman, M. A. C., Brown, A. G. A., Lebreton, Y., et al. 1998, *A&A*, 331, 81.
<https://arxiv.org/abs/astro-ph/9707253>
- Pinfield, D. J., Jameson, R. F., & Hodgkin, S. T. 1998, *MNRAS*, 299, 955, doi: [10.1046/j.1365-8711.1998.01754.x](https://doi.org/10.1046/j.1365-8711.1998.01754.x)
- Prosser, C. F. 1992, *AJ*, 103, 488, doi: [10.1086/116077](https://doi.org/10.1086/116077)
- . 1994, *AJ*, 107, 1422, doi: [10.1086/116955](https://doi.org/10.1086/116955)
- Prosser, C. F., Randich, S., Stauffer, J. R., Schmitt, J. H. M. M., & Simon, T. 1996, *AJ*, 112, 1570, doi: [10.1086/118124](https://doi.org/10.1086/118124)
- Proszkow, E.-M., Adams, F. C., Hartmann, L. W., & Tobin, J. J. 2009, *ApJ*, 697, 1020, doi: [10.1088/0004-637X/697/2/1020](https://doi.org/10.1088/0004-637X/697/2/1020)
- Raboud, D., & Mermilliod, J. C. 1998, *A&A*, 329, 101, doi: [10.48550/arXiv.astro-ph/9708144](https://doi.org/10.48550/arXiv.astro-ph/9708144)
- Robichon, N., Arenou, F., Mermilliod, J. C., & Turon, C. 1999, *A&A*, 345, 471, doi: [10.48550/arXiv.astro-ph/9903131](https://doi.org/10.48550/arXiv.astro-ph/9903131)
- Röser, S., Schilbach, E., Piskunov, A. E., Kharchenko, N. V., & Scholz, R. D. 2011, *A&A*, 531, A92, doi: [10.1051/0004-6361/201116948](https://doi.org/10.1051/0004-6361/201116948)
- Soderblom, D. R., Nelan, E., Benedict, G. F., et al. 2005, *AJ*, 129, 1616, doi: [10.1086/427860](https://doi.org/10.1086/427860)
- Southworth, J., Maxted, P. F. L., & Smalley, B. 2005, *A&A*, 429, 645, doi: [10.1051/0004-6361:20041867](https://doi.org/10.1051/0004-6361:20041867)
- Stauffer, J. R., Hartmann, L. W., & Jones, B. F. 1989, *ApJ*, 346, 160, doi: [10.1086/167996](https://doi.org/10.1086/167996)
- Taylor, B. J. 2006, *AJ*, 132, 2453, doi: [10.1086/508610](https://doi.org/10.1086/508610)
- van Leeuwen, F. 2009, *A&A*, 497, 209, doi: [10.1051/0004-6361/200811382](https://doi.org/10.1051/0004-6361/200811382)
- van Leeuwen, F., Le Poole, R. S., Reijns, R. A., Freeman, K. C., & de Zeeuw, P. T. 2000, *A&A*, 360, 472
- Vandenberg, D. A., & Bridges, T. J. 1984, *ApJ*, 278, 679, doi: [10.1086/161836](https://doi.org/10.1086/161836)
- Vereshchagin, S. V., & Chupina, N. V. 2013, *AN*, 334, 892, doi: [10.1002/asna.201311938](https://doi.org/10.1002/asna.201311938)
- Vereshchagin, S. V., Reva, V. G., & Chupina, N. V. 2013, *ARep*, 57, 52, doi: [10.1134/S1063772912120062](https://doi.org/10.1134/S1063772912120062)
- Zuckerman, B., Melis, C., Rhee, J. H., Schneider, A., & Song, I. 2012, *ApJ*, 752, 58, doi: [10.1088/0004-637X/752/1/58](https://doi.org/10.1088/0004-637X/752/1/58)